A STUDY OF
FULLY DEVELOPED TURBULENT FLOW
AT A VERY HIGH REYNOLDS NUMBER

By

Masahiro Nagashi

1931

Guggenheim Graduate School of Aeronautics
California Institute of Technology
Pasadena, California

CONTENTS

SUMMARY OF EXPERIMENT

In the present experiment, a study of a completely developed turbulent flow at Reynolds Number 700,000 was made, using a long circular tube of 38 cm. in diameter, through which air was drawn by a propeller type fan. The Pitot tube method of measurement was employed.

The pressure drop along the channel at the wall and also at the axis of the tunnel was measured, and from this the wall friction and the shearing stresses in the flow were determined and plotted. Velocity distributions at 11 sections approximately equally spaced were measured and plotted on the same sheet for comparison. It was found that the velocity distribution near the entrance was very much distorted, but after 10 diameters the distortion had vanished. At this point the flow had the fully developed turbulent characteristics.

The measurement of the fully developed turbulence was made at the sections 21.57 and 23 diameters from the entrance. Velocity distributions very near the wall as well as all the way across the section were obtained, and from these the exponent of velocity distribution was determined to be 9.6. This value was found to fall on the curve drawn through the points obtained by Nikuradse and Möbius in their experiments. Mischungsweg distributions using both Prandtl's ($\frac{1}{r} = \frac{\sqrt{\frac{\tau}{\rho}}}{r\frac{du}{dy}}$) and von Kármán's ($\frac{1}{r} = \frac{\kappa}{r}\frac{\frac{du}{dy}}{\frac{d^2u}{dy^2}}$) formulae were also calculated and plotted. The two curves agree well near the wall, but Kármán's curve lies quite a distance below Prandtl's curve for the points toward the center of the tube. The Kármán Formula ($\frac{1}{r} = 2\kappa\left\{\sqrt{1-\frac{y_1}{r}} + \frac{y_1}{r} - 1\right.$) gives a curve that lies approximately half way between the above two curves.

OBJECT AND SCOPE OF THE EXPERIMENT

The object of this experiment is to make a study of a fully developed turbulent flow at a very high Reynolds Number, using a large circular tube, through which air was drawn. In determining the behavior of the air stream, Pitot tubes were used in the present experiment. This investigation is a preliminary study of the turbulence and other characteristics of the tunnel for the subsequent experiment to be conducted by Mr. A. M. Kuethe of the California Institute of Technology. In the subsequent experiment, a direct measurement of the eddying motion and a determination of the values of mischungsweg distribution of the turbulent flow will be made at the same measuring sections in the same tunnel, using an electric anemometer and oscillograph method.

The following studies were made in this experiment:

1) Velocity distribution of the flow at eleven different measuring sections of the tunnel.
2) Determination of the pressure drop in the tunnel.
3) Determination of the shearing stress of the flow.
4) Measurement of the velocity distribution of the completely turbulent flow near the wall as well as all the way across the section, at R= 700,000.
5) Determination of the power law at this R.
6) Rough study of the effects of different entrance conditions upon the developement of the turbulence.
7) Determination of the mischungsweg distribution of the completely developed turbulent flow at this R.

INTRODUCTION

In an ideal, that is incompressible, non viscous fluid, a body in motion does not experience any resistance, but in a real fluid, such as air which has viscous properties, it offers resistance, and from this frictional drag, a boundary layer is built up about the body in motion. In the study of aircraft, this resistance is of extreme importance, as it causes the craft to behave differently than it would in an ideal non-viscous fluid. Experiments show that there are two kinds of boundary layers, namely: laminar and turbulent. The laminar boundary layer is that part of air flow affected by the resistance of the body surface having its flow approximately parallel with the surface, while the turbulent boundary layer is that boundary layer in which the flow does not have any definite direction and is eddying.

When the speed of the aircraft is slow and the size small, the boundary layer is more likely to be laminar than turbulent, but at a high speed, the boundary layer becomes turbulent, and the behavior of the boundary layer, and hence its study becomes an important subject.

A considerable amount of work has been done on the flow of air at low speeds or at low Reynolds Numbers, in which the boundary layer is laminar, but so far very little work has been done on the turbulent boundary layer which usually occurs at high Reynolds Numbers.

In the study of the turbulent boundary layer, because of the irregularities of flow, difficulty of formulating a

general theory has been met and as yet there is no theory which expresses the turbulent flow completely. Many of the expressions which have been worked out are semi-empirical in form and a considerable amount of experimental investigation must yet be carried out before a complete theory can be formulated.

For the investigation of turbulence, flow of fluids in channels, both two and three dimensional, have been studied, particularly by Nikuradse (Ref. 7) and Dönch (Ref. 8) and boundary layer on flat plates by Hansen (Ref. 9) and van der Hegge Zijnen (Ref. 10).

When an undisturbed flow of an incompressible viscous fluid comes in contact with a solid surface, the layer very close to the surface tends to adhere to it, and offers resistance to the motion. This resisting force is transmitted to the adjoining layer, retarding its velocity until the force is entirely consumed in the retardation of the fluid motion. Beyond this point out from the wall, the flow is undisturbed and is potential. The velocity distribution curve very near the wall regardless of the speed and Reynolds Number ($R = \frac{UD}{\nu}$) is laminar and is roughly parabolic in shape. W. Tollmien (Ref. 11) found theoretically that if the Reynolds Number ($R^* = \frac{U\delta}{\nu}$) where U is the velocity of undisturbed flow, δ is the boundary layer thickness from the wall and ν is the coefficient of kinematic viscosity, is lower than 1230 approximately, the boundary layer is laminar and its shape is hence approximately parabolic. This value is the lowest limit of the critical Reynolds Number for turbulent boundary layer, and

by constantly decreasing the initial disturbing conditions of the flow, an upper limit of Reynolds Number of 20,000 has even been reached in an experiment by Schiller without changing the laminar layer to a turbulent layer.

When in a channel the Reynolds Number R* is below the critical point for the particular flow, the boundary layer remains laminar, and its thickness increases until it meets with the thickening layer from the opposite wall forming a completely parabolic velocity distribution curve across the channel.

However, when the Reynolds Number R* or R is increased beyond its critical point, the flow suddenly becomes turbulent, and a turbulent boundary layer forms. Then the velocity distribution curve of the flow assumes a different shape. The shape of the velocity distribution curve is known to be a function of distance from the wall and also of Reynolds Number, and may be written (Ref. 13) $u \backsim y^{\frac{1}{n}}$ where u is the local velocity, y the distance from the wall, and n the power coefficient. The value of n increases from 7 to 10 as the Reynolds Number is increased, according to the experiments so far performed. (Ref. 12 and 21). The turbulent boundary layer after its formation grows in thickness until, just as in the case of the laminar boundary layer, it meets with the thickening layer from the opposite wall. Thence the flow remains completely turbulent throughout the section, and the shape of the velocity distribution curve remains unchanged until the shape of the channel is changed or some disturbance

is introduced so as to change the flow. The present investigation was made in this completely turbulent region.

PREVIOUS EXPERIMENTS

Stanton and Pannel (Ref. 17) studied the velocity distribution of turbulent flow using pipes of various diameters from .3 to 10 cm. and velocities varying from 30-6000 cm./sec.. The fluids used were air and water and the range of Reynolds Numbers was $R = \frac{U D}{\nu} = 2500$ to 430,000. They observed and plotted the surface resistance against Reynolds Number using the relation

$$R_0 = U^2 \rho f\left(\frac{U D}{\nu}\right)$$

where, R_0---resistance,
U---velocity at the axis of the channel,
ρ---density of the fluid,
D---diameter of the channel,
ν---coefficient of kinematic viscosity.

They concluded that,

1) The velocity distribution is independent of the values of the Reynolds Number only when the surfaces of the pipes are so roughened that the resistance varies as the square of the velocity.

2) The critical Reynolds Number for a laminar flow in a pipe to become a turbulent flow is about 2500, and during the transition, the resistance suddenly increases.

J. Nikuradse, using glass Pitot tubes and a specially devised photographic apparatus measured the velocity distribution in a circular, a triangular and an open rectangular channel. In the circular and the triangular channels water under pressure was run through, and velocities of 800 and 1200 cm./sec. respectively were obtained. The Reynolds Numbers reached were

172,000 for the circular channel and 156,000 for the triangular channel. In the range of Reynolds Numbers investigated the Prandtl-Kármán 1/7 power law was satisfied in all the three cases, and the Kármán's numerical constant "k" was also verified quite exactly. The Reynolds Number used here was defined by

$$R = \frac{\bar{U} L}{\nu}$$

where, $\bar{U}$---mean velocity,
L---hydraulic diameter,
F---cross sectional area.

$$L = \frac{4 F}{\text{periphery}}$$

Dönch in 1926 (Ref. 8) took measurements using a rectangular wooden channel of the following dimensions: length 700 cm., height 65 cm., breadth 15 cm.. Using air as fluid, he obtained a velocity of 1100 cm./sec. and R = 180,000 by means of a four bladed propeller run by an electric motor. His curves for apparent resistance agree quite well with those obtained by Nikuradse when various different experimental conditions are taken into consideration. Dönch states that the Prandtl 1/7 power law of velocity distribution for the region of Reynolds Number of this experiment does not quite agree with his values, and suggests the use of 1/8 power law.

However, according to an experiment performed by Nikuradse in 1929, (Ref. 7) using water as fluid, and a very narrow and deep channel, he found that atthe Reynolds Number of 67,000, Prandtl's 1/7 power law works well instead of Dönch's 1/8 power law.

Nikuradse performed another experiment (Ref. 20) using water under a high pressure in which by warming the water, he obtained a Reynolds Number as high as 900,000. The water under the high pressure was discharged at a very high speed, and by

the warming its coefficient of kinematic viscosity was decreased so that the value of Reynolds Number was increased. Velocity distribution at 40, 65, and 100 diameters from the entrance were plotted on the same sheet, and were found to coincide exactly, showing that the velocity distribution, after the flow becomes completely turbulent, remains unchanged. He plotted the resistance coefficient $\lambda = \frac{dP}{dx} \frac{d}{\bar{q}}$ (where dp/dx is the pressure gradient along the tunnel axis, d the diameter of the pipe and $\bar{q}$ the dynamic head) against Reynolds Number, and found that the points lie on the line drawn through the points determined by former workers, but below the extrapolated Lee's formula, $\lambda = .00714 - .614\ R^{-.36}$

Hopf (Ref. 22) collected and analyzed the results of numberous researches on pipes of various materials. He found that they can be classified into two distinct types, according to the form of resistance curve given. He found that the pipes of medium roughness (rough iron, cement etc. walls)give a pressure drop proportional to the square of the velocity, while pipes having a smooth undulating surface (e.g. walls of wood, sheet iron etc.) give a pressure drop almost parallel to the smooth Blasius curve.

Fromm (Ref. 22) investigated the pressure drop for a channel having serrated walls i.e. the surface of a wall of saw like profile, and found that it is possible to obtain a pressure drop proportional to a power greater than the square of the velocity. Theoretically it is difficult to understand this phenomenon obtained by Fromm. Probably in his case the turbulent flow was not fully developed and was in a transitional stage.

Fritsch (Ref. 23) investigated the flow in channels having rough walls keeping the quantity of flow constant and varying the velocity profiles by changing the wall conditions, and found that there is very little similarity between the distribution of speed. However, when comparison of the distributions was made for equal pressure drop conditions, then the profiles of velocity in the center of the channel were found to be congruent, verifying the Prandtl-Kármán assumption that the velocity distribution in turbulent flow depends on the wall friction alone. Fritsch also found that the mischungsweg distribution is practically the same for smooth, rough and undulating walls.

Jacob and Erk (Ref. 21) and subsequent workers have shown that Blasius' law of 1/7 power holds up to about R=100,0 but that beyond this value the value of n would increase to n = 8, 9, 10 etc. according to the magnitude of Reynolds Numbers.

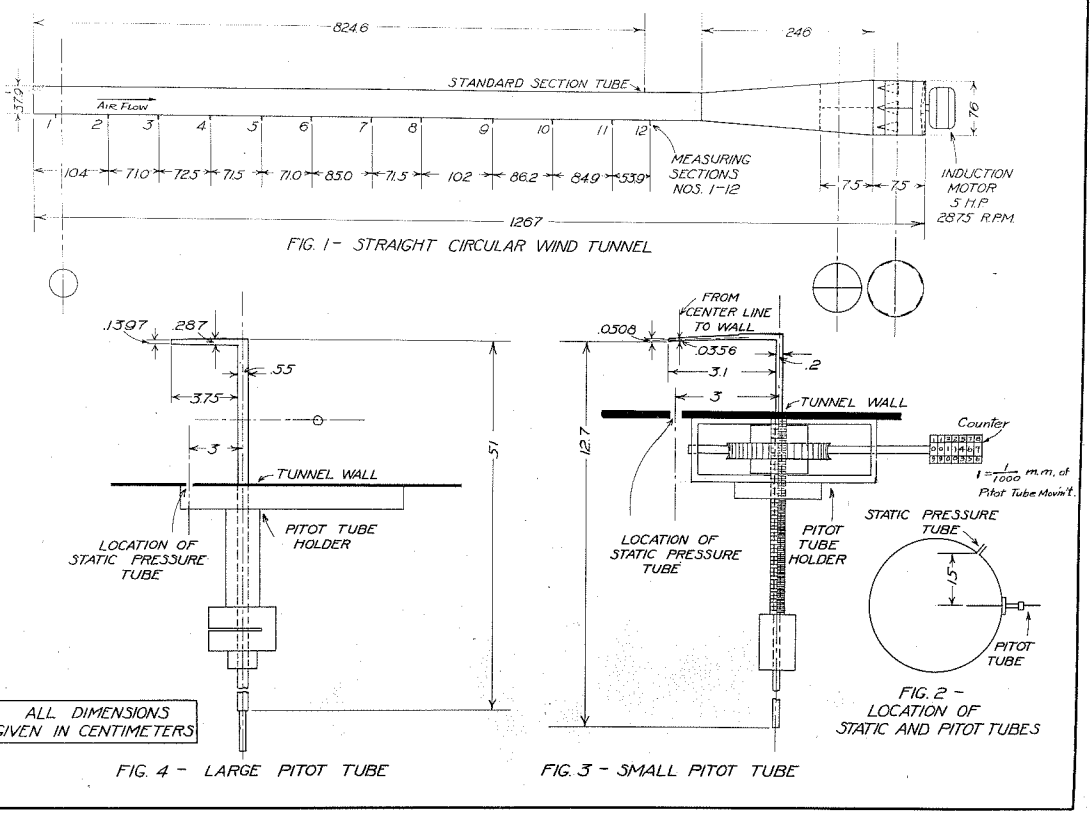

FIG. 1 - STRAIGHT CIRCULAR WIND TUNNEL

FIG. 4 - LARGE PITOT TUBE

FIG. 3 - SMALL PITOT TUBE

FIG. 2 - LOCATION OF STATIC AND PITOT TUBES

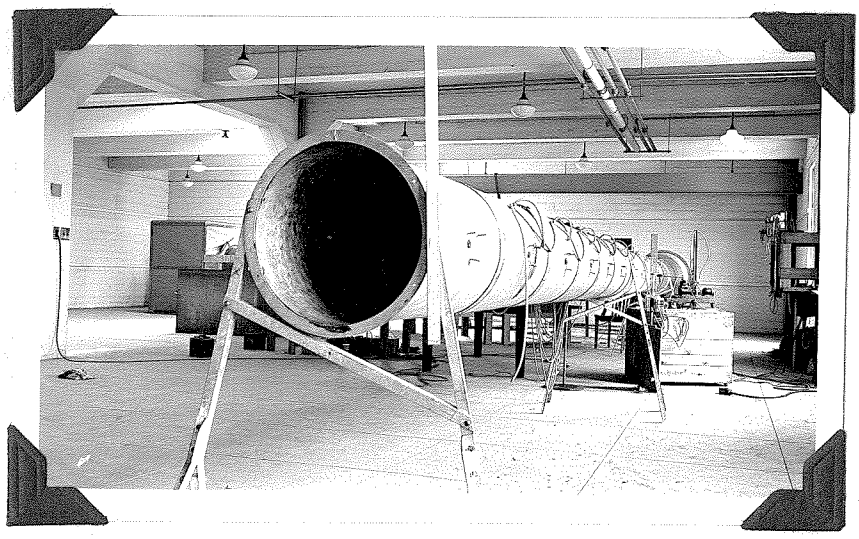

Fig. 5

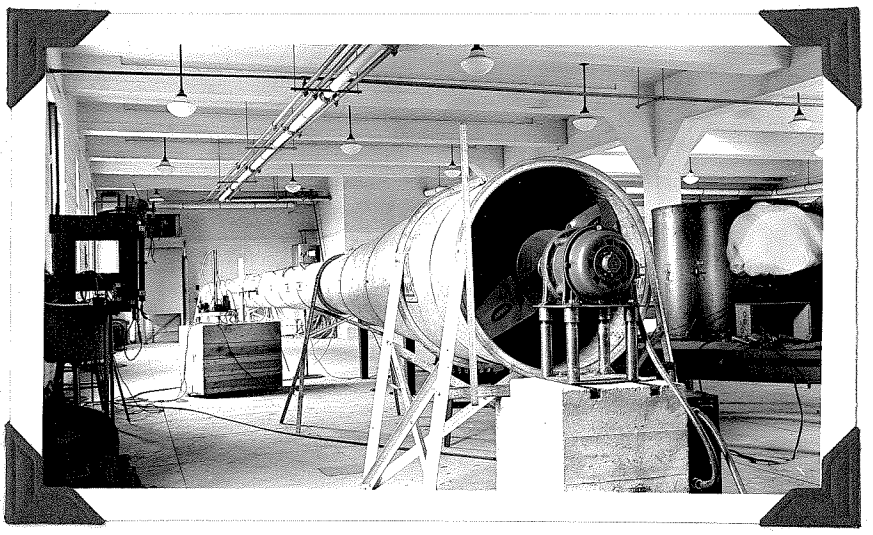

Fig. 6

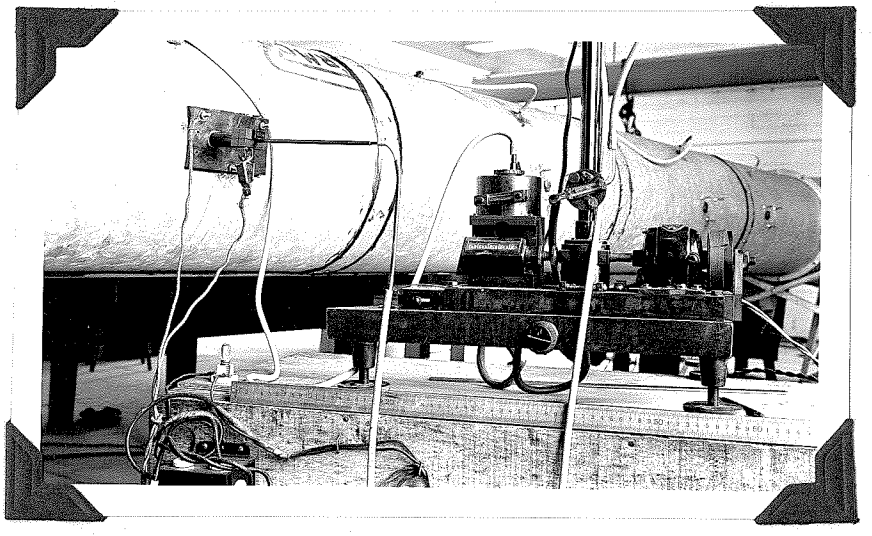

Fig. 7

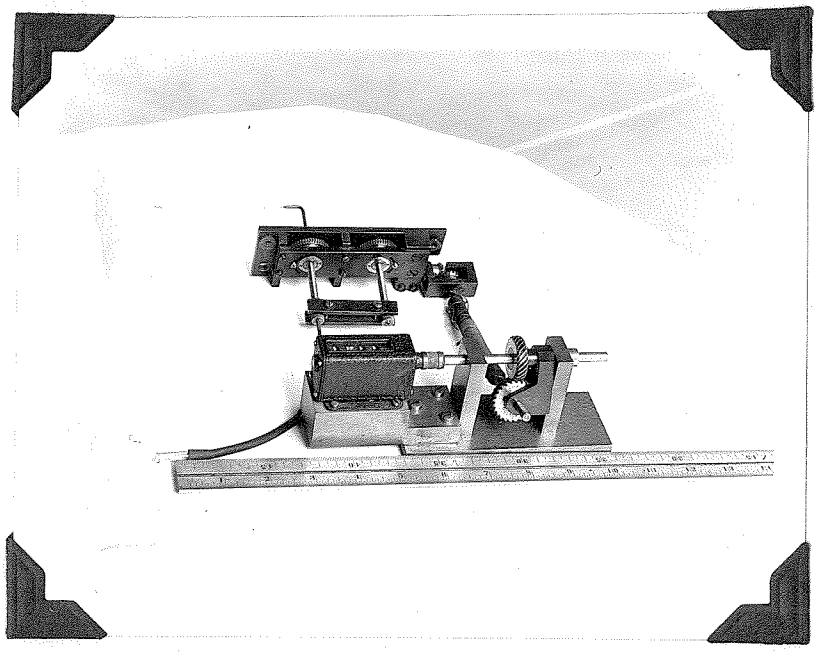

Fig. 8

APPARATUS

Wind Tunnel

For the measurement of the turbulent flow, a wind tunnel of circular section of inside diameter 38 cm. (varying between 37.9-38.1 cm.) and of length of 1267 cm. was used. The tunnel was constructed of sheet metal rivetted at the joints and tightly sealed with sealing wax to avoid any air leakage. As shown in the Fig. 1, the tunnel is tapered out from the parallel section to the outlet end, where a 2875 r.p.m. 5 h.p. induction motor was placed for air suction. The propeller was especially designed for this motor and the tunnel by Dr. Troller of Guggenheim Airship Institute. Near the outlet end, several adjustable triangular openings were provided for the regulation of the tunnel's air speed. (Figs. 1 & 6). The measuring sections were chosen at points approximately half way between the tunnel joints so as to avoid local disturbances. A point 824.6 cm. from the inlet end of the tunnel was taken to be the standard section, and the measurement for the airflow regulation was made at this point throughout the entire experiment.

Pitot Tubes and Micrometer

Two Pitot tubes of different sizes were used. One as shown in Fig. 4 and in the upper left hand corner of Fig. 7, was used for the measurement of velocity distribution over the tunnel section from a point approximately .5 cm. out from its wall; and the other as shown in Figs. 3, 8 and 9, attached to a micrometer, was used to measure the boundary layer very

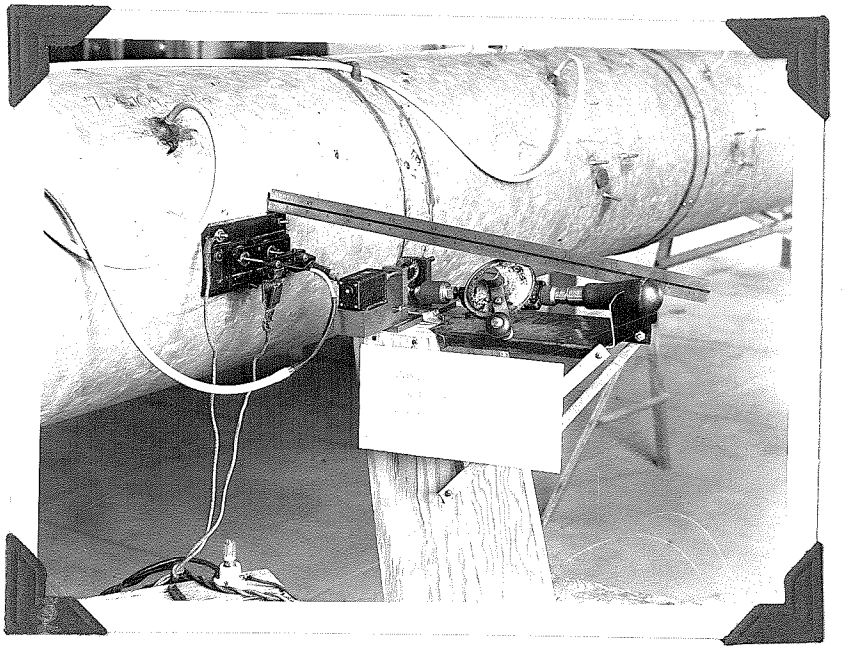

Fig. 9

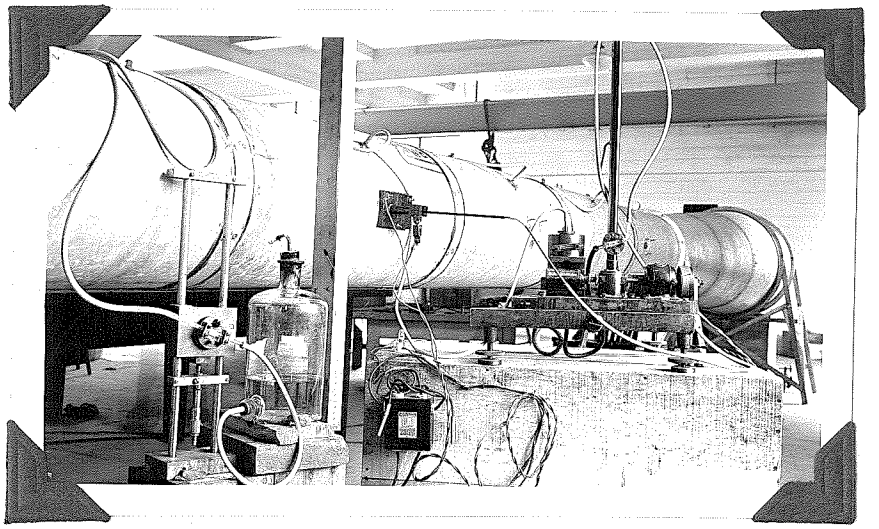

Fig. 10

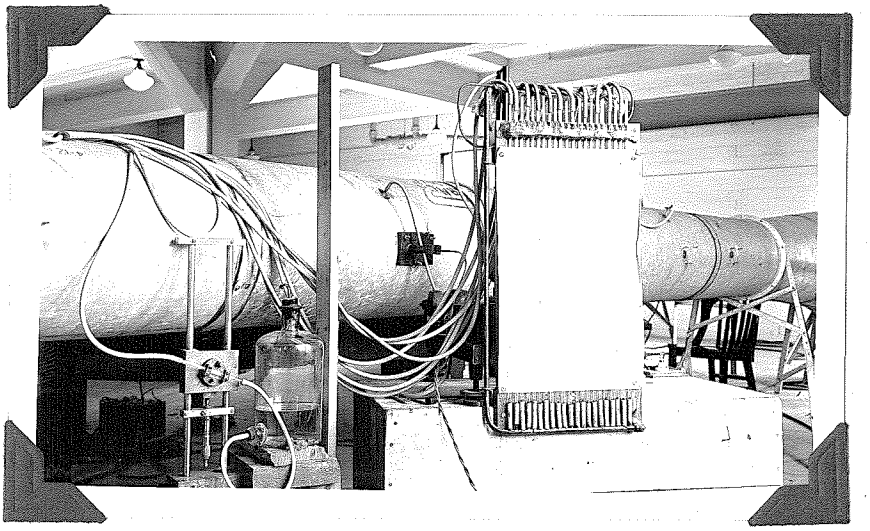

Fig. 11

near the wall, namely, .0356 to 1.4 cm. from the wall. The micrometer was designed to measure the movement of the Pitot tube to .0001 cm. but due to constructional difficulty, the accuracy of the micrometer can be taken to be only .002 cm. of the Pitot tube movement. The measurement of the location of the large Pitot tube was made by measuring by means of a steel scale, the distance of a mark on the tube from the tunnel wall. This method of measurement may be considered to be accurate to .03 cm.

The contact point of the tube to the tunnel wall was determined by means of an electric circuit, so devised that when the tube came in contact with the tunnel wall a light globe as shown at the lower left hand corner of Figs. 7 and 9, lighted. The readings of the Pitot tube position were taken from this contact point.

The static pressure was measured by means of a series of static tubes, each .2 cm. in diameter and approximately 2 cm. in length, attached flush to the inside surface of the tunnel wall. The holes were carefully drilled and the inside surface carefully smoothed by scraping, in order to avoid any error in measurement from protruding scales in the tunnel wall caused by drilling.

The method of attaching the Pitot tube to the tunnel was as follows:

Pitot tube holders were constructed to fit the tubes, and attached to the tunnel by means of three screws which were solidly soldered to the outside surface of the tunnel. The positions of the Pitot tube and the static tube are

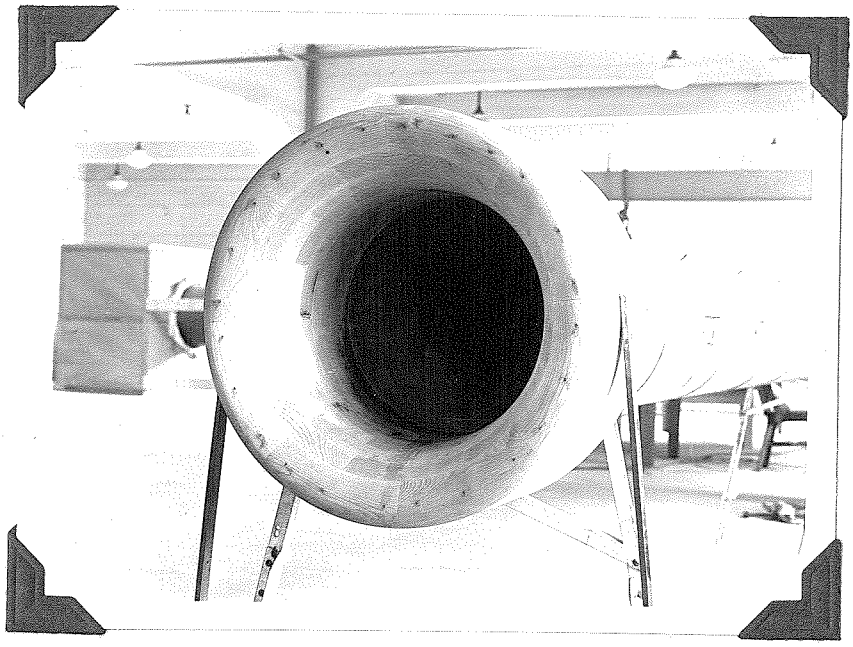

Fig. 12

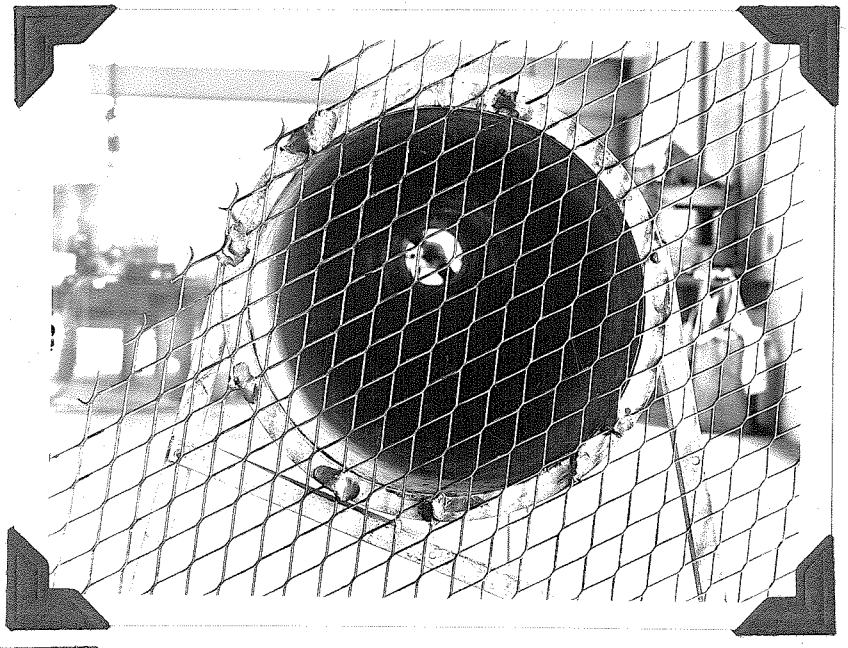

Fig. 13

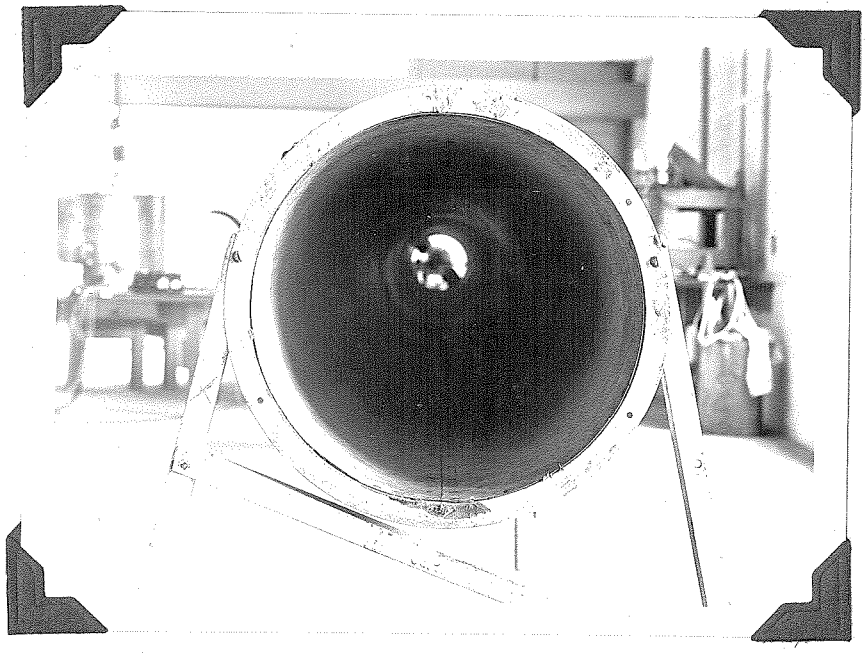

Fig. 14

shown in Figs. 2, 3 and 5.

Manometers.

1) For the measurement of the velocity distribution, a motor dirven, inclined tube, N.A.C.A. type micromanometer using ethylene chlorohydrin (CH_2 (OH) CH_2 Cl) was used. This manometer measured to .001 cm. of the pressure height of the fluid.

2) A "U" tube type multiple manometer as shown in Fig. 11 was used for measuring the static pressure drop of the tunnel. The measurement was made in darkness by shining a bright light upon a sensitized paper placed behind the tubes while the tunnel was being run. The manometer and the static tubes were connected with rubber tubings. Alcohol was used in this manometer.

3) In order to measure the speed for the maintanance of a constant airflow, another manometer as shwon in the lower left hand corner of Figs 10 and 11 was used, and by means of a rubber tubing it was connected with a static pressure tube at the standard section. Alcohol was used in the manometer.

Diagram 1

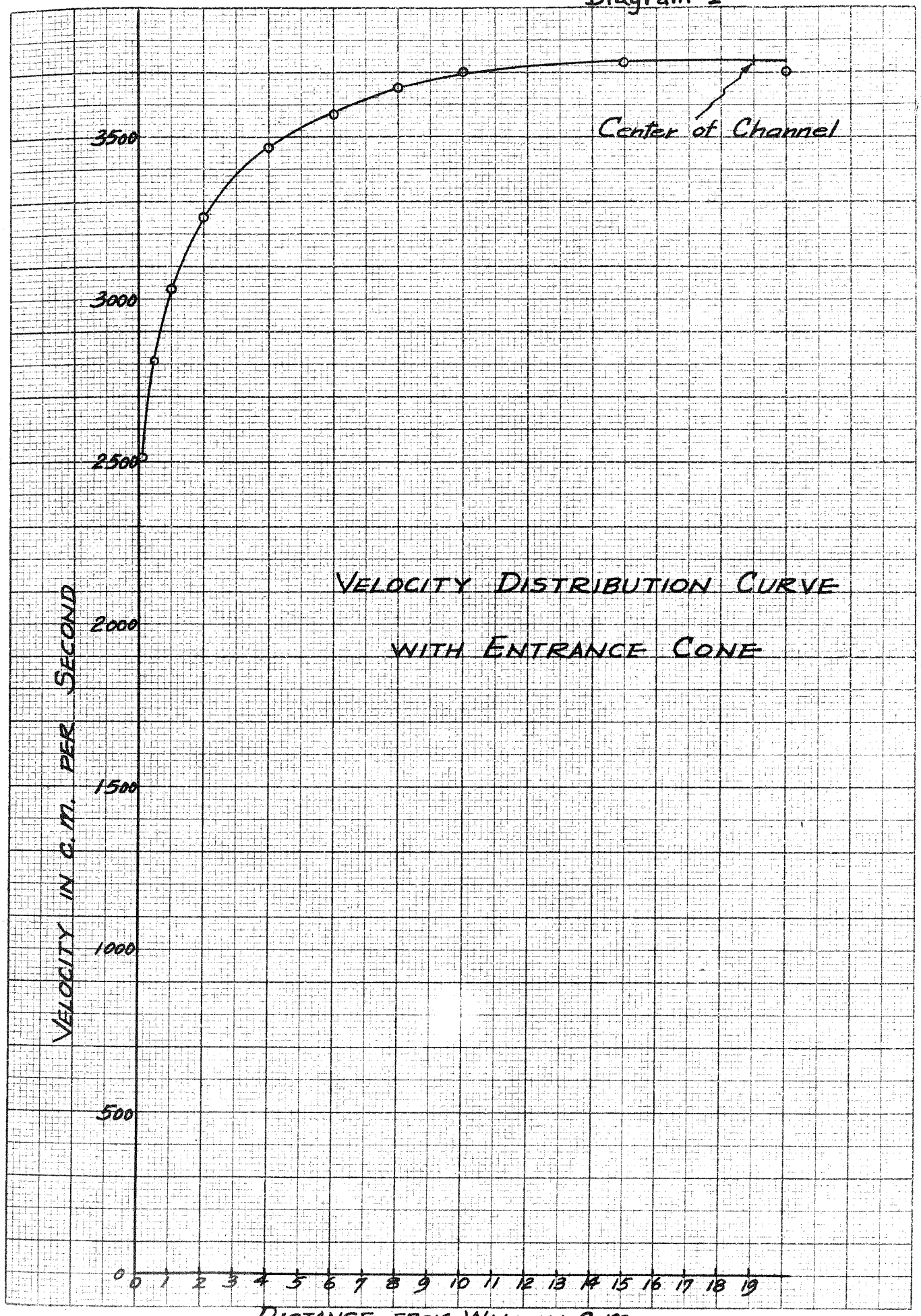

VELOCITY DISTRIBUTION CURVE

WITH ENTRANCE CONE

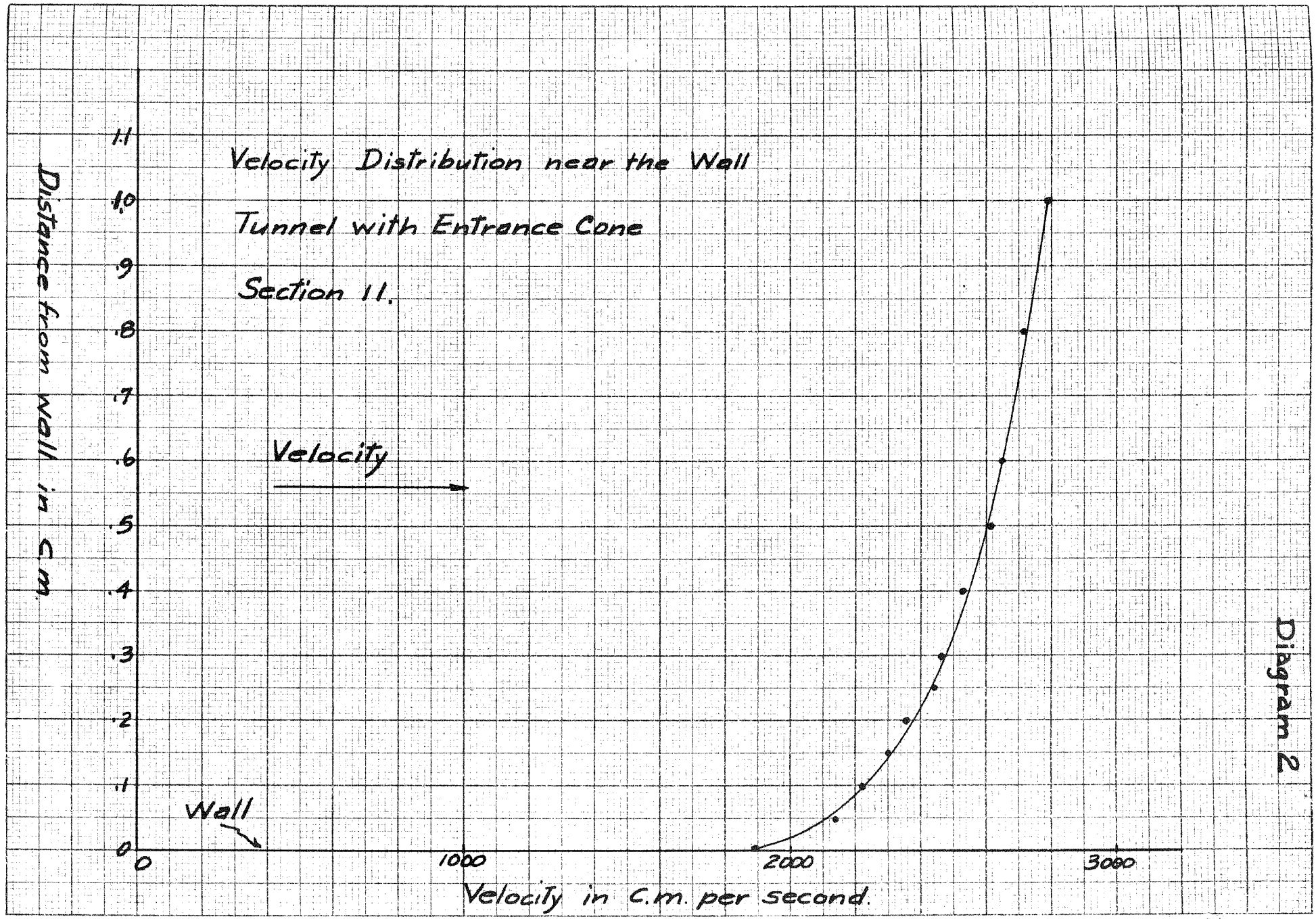
Velocity Distribution near the Wall
Tunnel with Entrance Cone
Section 11.
Velocity
Wall
Distance from wall in C.m.
1.1
1.0
.9
.8
.7
.6
.5
.4
.3
.2
.1
0
0
1000
2000
3000
Velocity in C.m. per second.
Diagram 2

Diagram 3

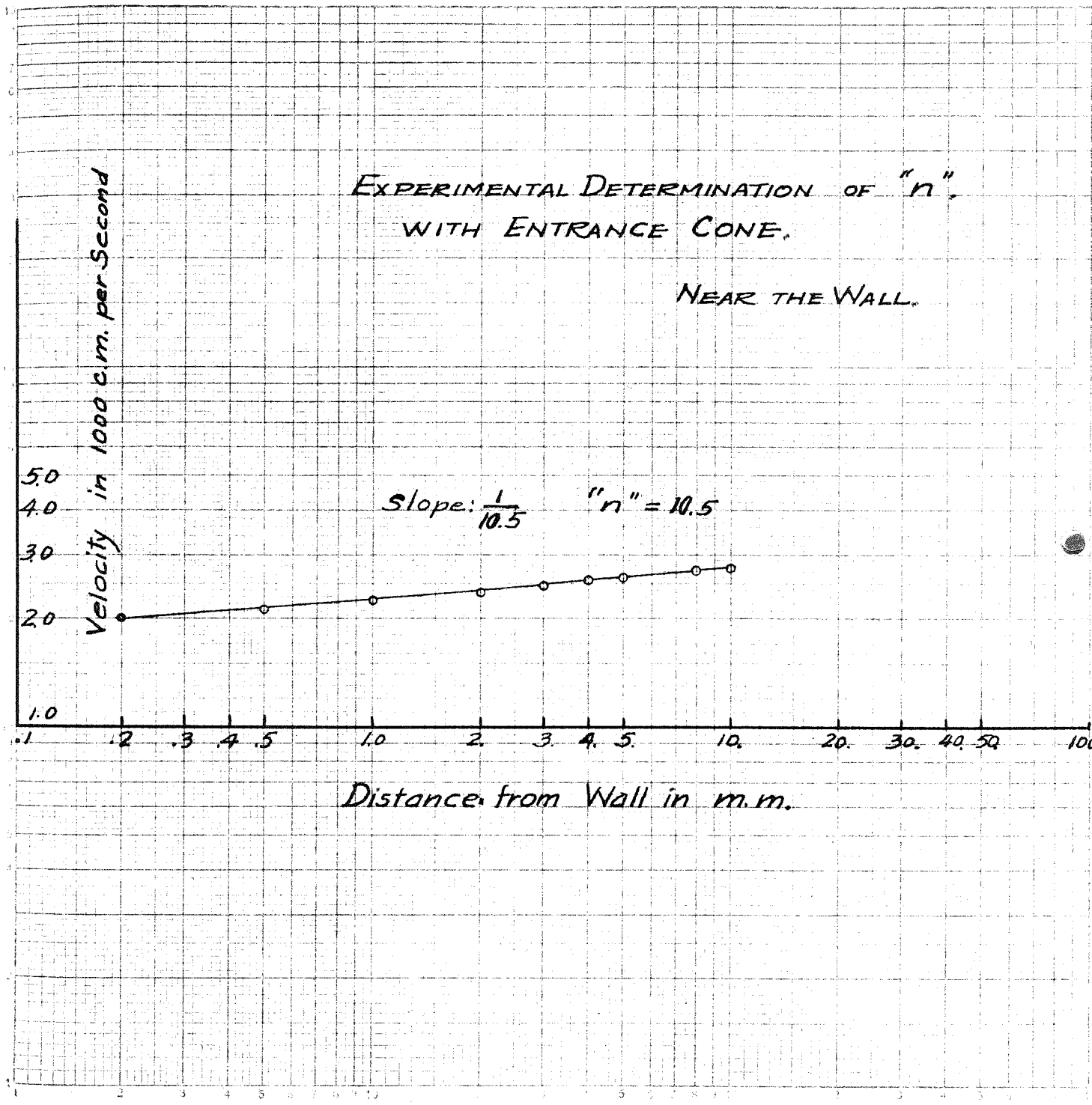

PRELIMINARY INVESTIGATION

Variation of Turbulence under Different Entrance Conditions

In order to determine whether the section 12 (Fig. 1) was sufficiently far back from the entrance to obtain a fully developed turbulent flow, a preliminary measurement under different entrance conditions was made.

(1) Stream Lined Entrance Cone

First a well shaped entrance cone, (Fig. 12) was attached to the tunnel, and the velocity distribution at the section 12 was measured with the motor running at its full speed. The velocity distribution at the center section was very flat, and from the appearance of the velocity distribution curve, a conclusion was reached that the boundary layers had not joined, although the boundary layer was turbulent. (Diagram 1, 2 and 3) Diag. 3 was plotted using the curve of the Diag. 2, and indicates that the value of the power coefficient "n" is 10.5 which is far greater than 2, which is the usual value of "n" for a laminar flow.

As the motor was run at its full speed, there was no way of increasing the Reynolds Number except by changing the tunnel or changing the motor. As the flow near the wall was turbulent, the boundary layers may be made to meet by lengthening the tunnel, or by employing some means by which the turbulence may be set up without decreasing the velocity materially. For this reason, in order to obtain a fully developed turbulence without lengthening the tunnel or changing the motor, different entrance conditions were tried as described in the following paragraphs.

Diagram 4

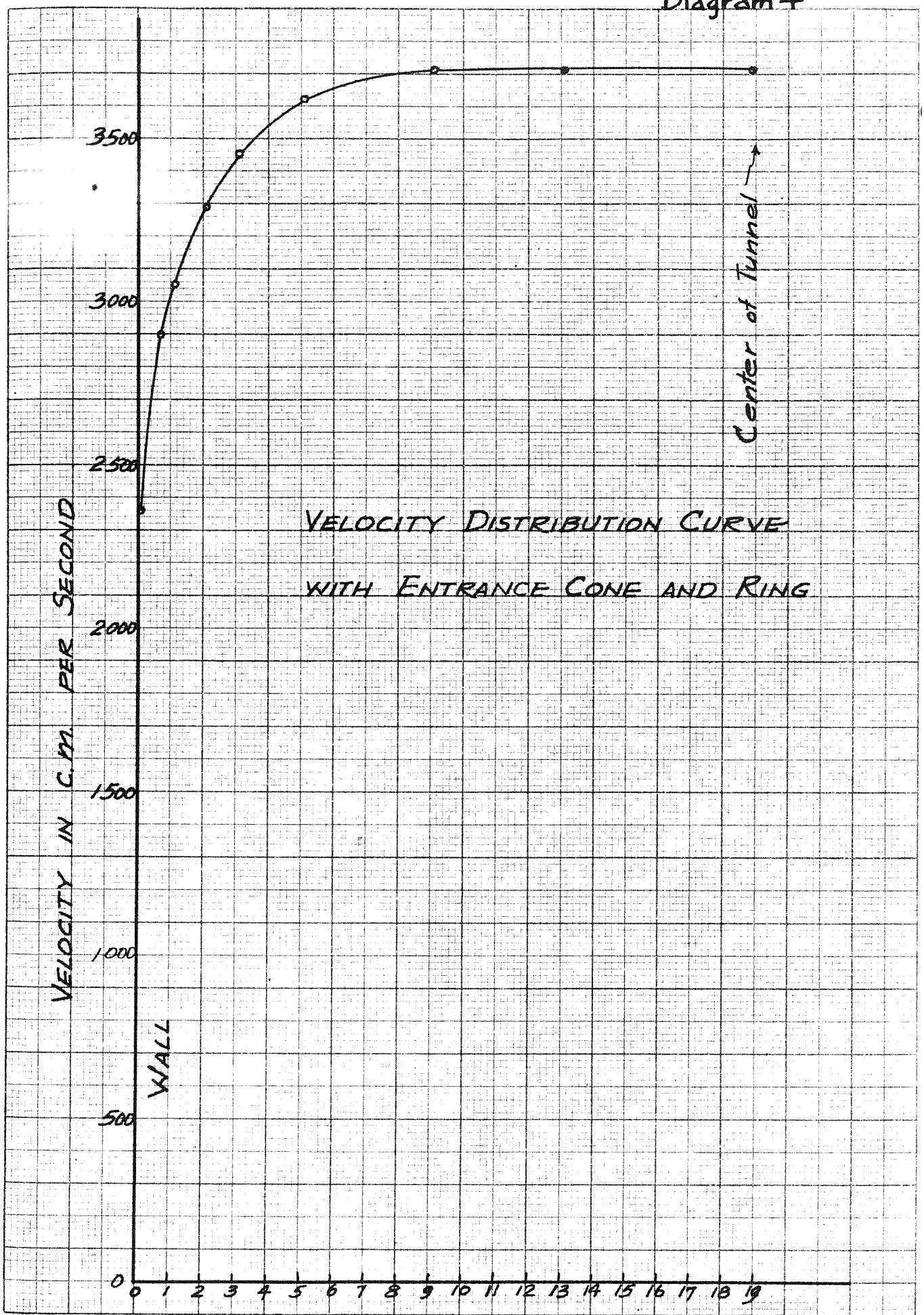

VELOCITY DISTRIBUTION CURVE

WITH ENTRANCE CONE AND RING

Diagram 5

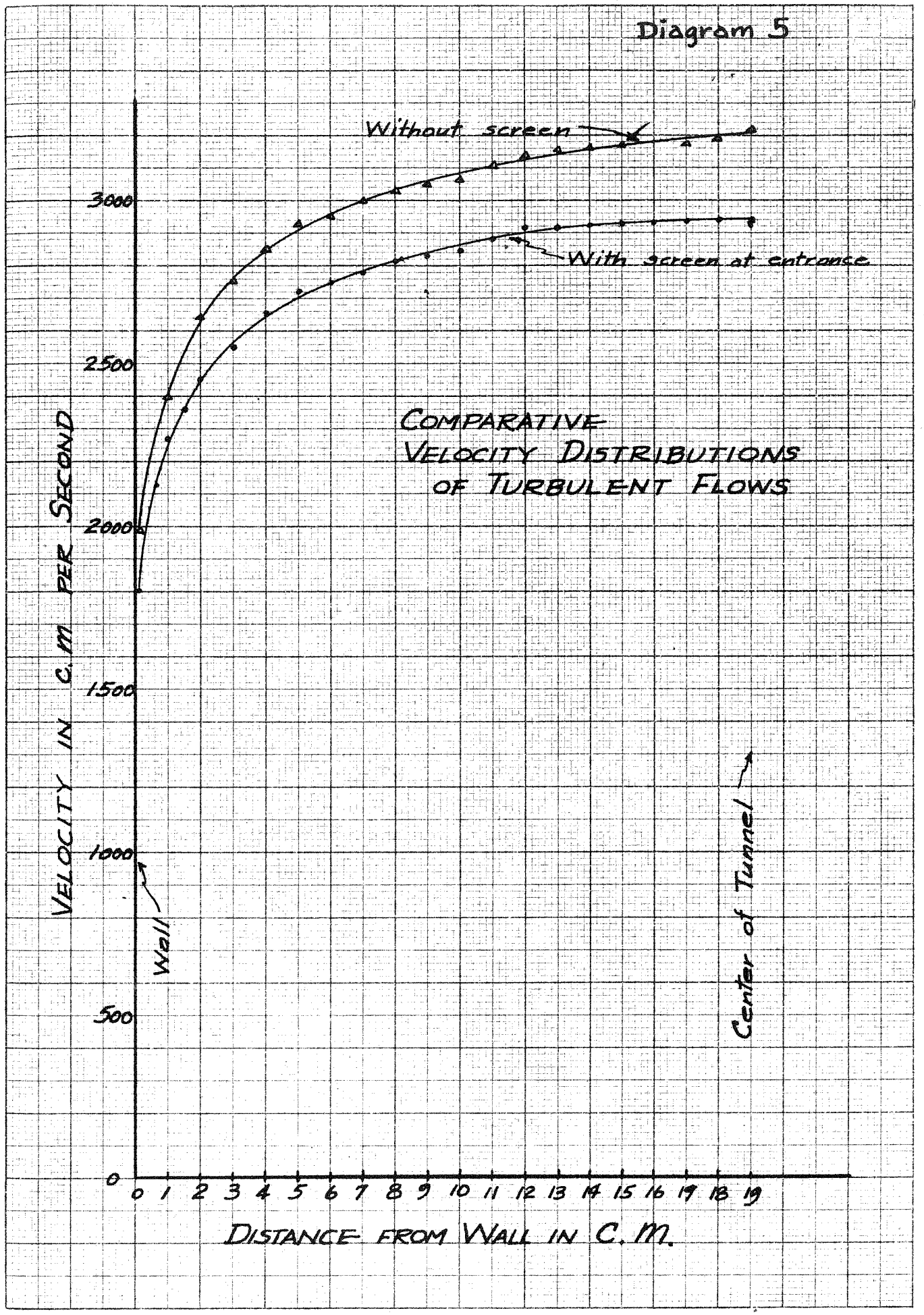

(2) Stream Lined Entrance Cone with a Ring Breaker

A ring made out of ¼ inch (diameter) copper tubing was attached on the inside of the cone at a point where the curvature of the cone straightens out parallel with the axis of the tunnel, and a measurement of the velocity distribution at the section 12 was taken. This decreased the maximum velocity of the air flow, but did not aid much to develope the required turbulence, and the velocity distribution at the section still was flat at the center of the tunnel section. (Diagram 4.)

(3) Screened Entrance

Next, the entrance cone was removed and a rough screen (Fig. 13) was placed at the entrance, and a measurement was taken. The result was plotted on Diag. 5. This again failed to bring about a completely developed turbulent flow.

(4) Sharp Entrance

Finally, the screen was removed leaving the entrance sharp and blunt as shown in the Fig. 14. The result of the measurement was plotted on the Diag. 5, together with the result of the measurement taken with screen at the entrance. The boundary layers apparently have joined, because the curve has no flat section as in the previous cases.

Determination of the Completely Developed Turbulence

The preceeding investigation was a rough determination and it was necessary to ascertain a little more carefully that the flow was completely turbulent throughout the section of the tunnel. To do this, the following methods were employed:

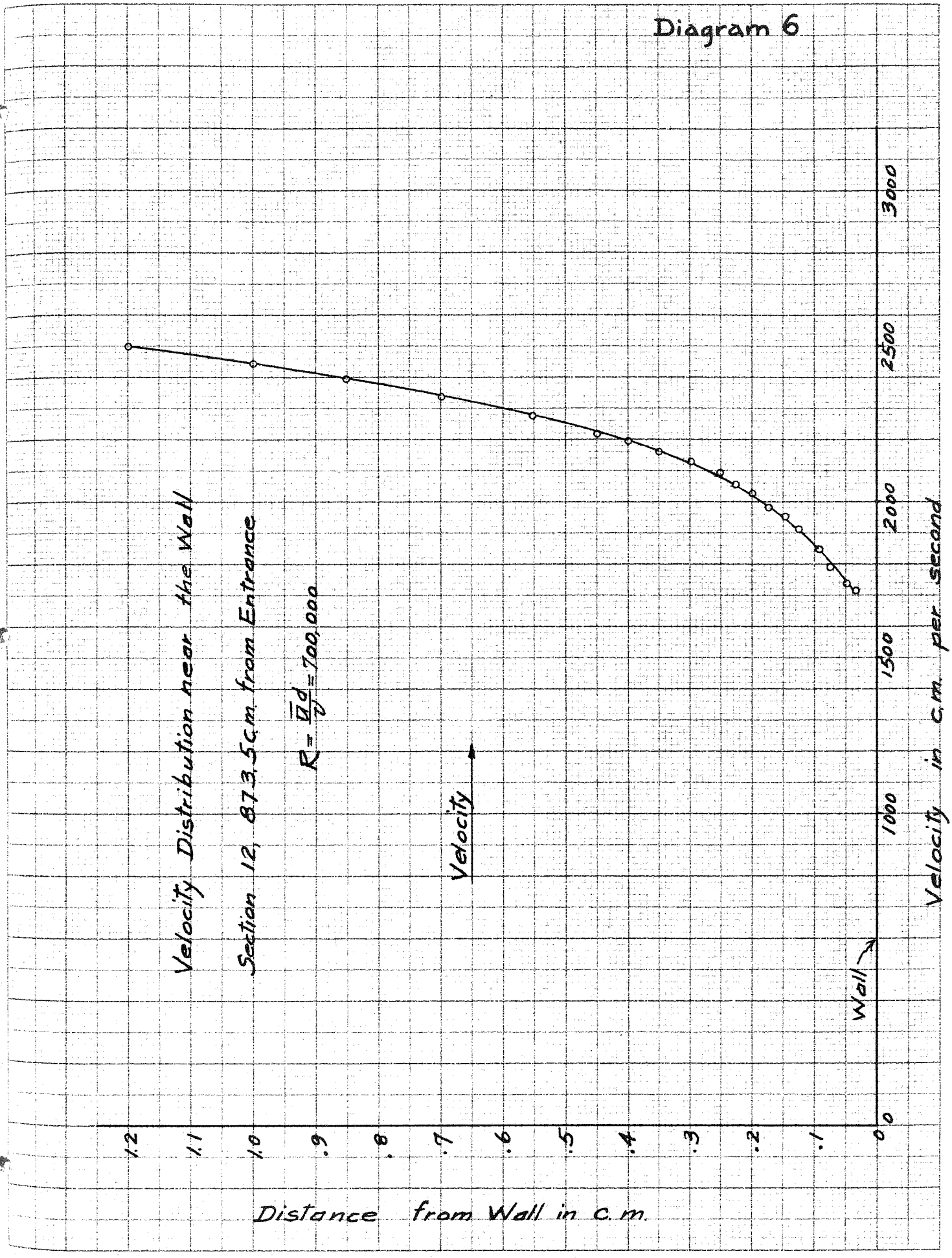
Diagram 6
Velocity Distribution near the Wall
Section 12, 873.5 c.m. from Entrance
$R = \frac{\bar{U}d}{\nu} = 700,000$
Velocity
Wall
Velocity in c.m. per second
0
1000
1500
2000
2500
3000
.1
.2
.3
.4
.5
.6
.7
.8
.9
1.0
1.1
1.2
Distance from Wall in c.m.

Diagram 7

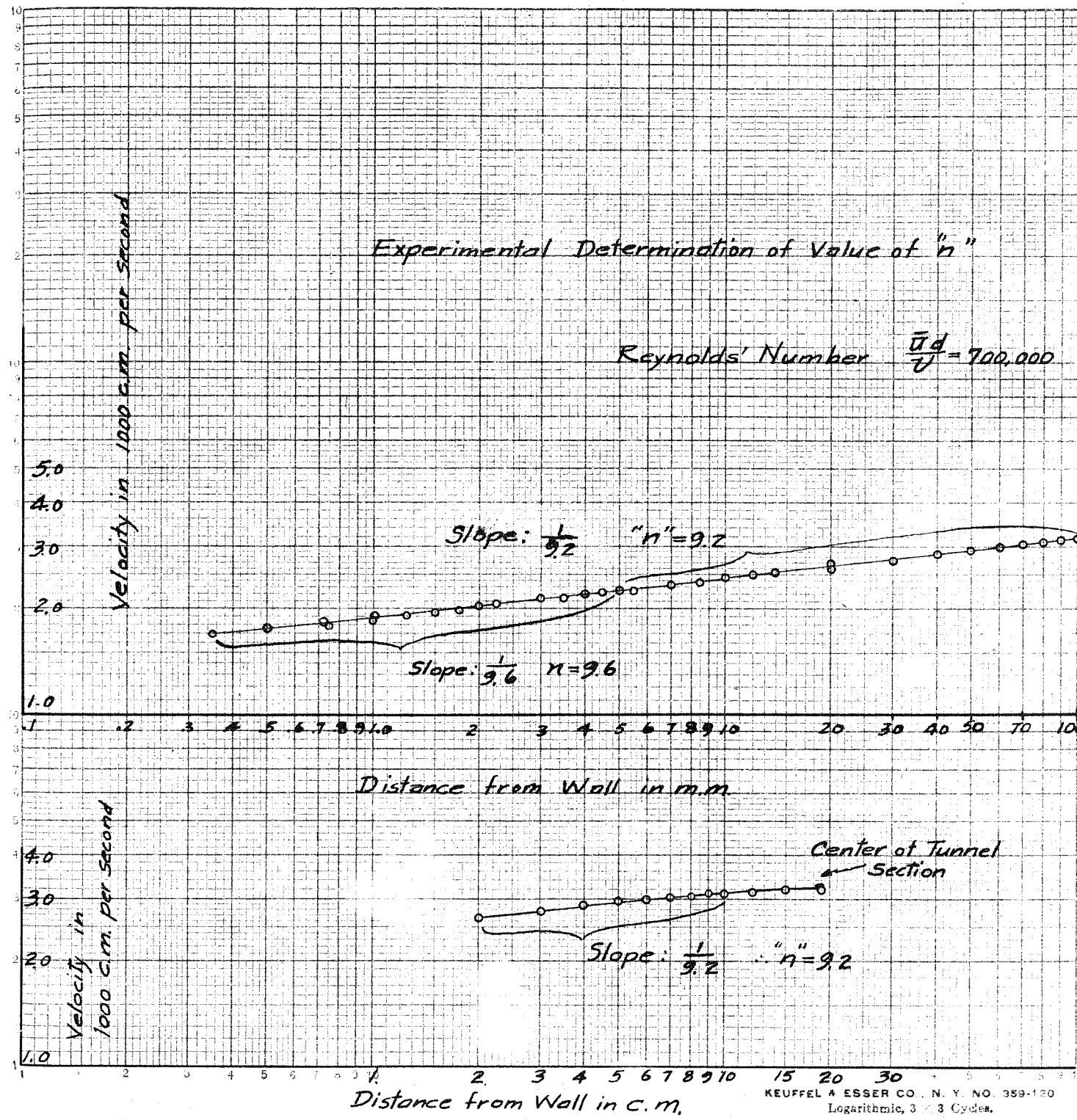

KEUFFEL & ESSER CO. N. Y. NO. 359-120
Logarithmic, 3 × 3 Cycles.

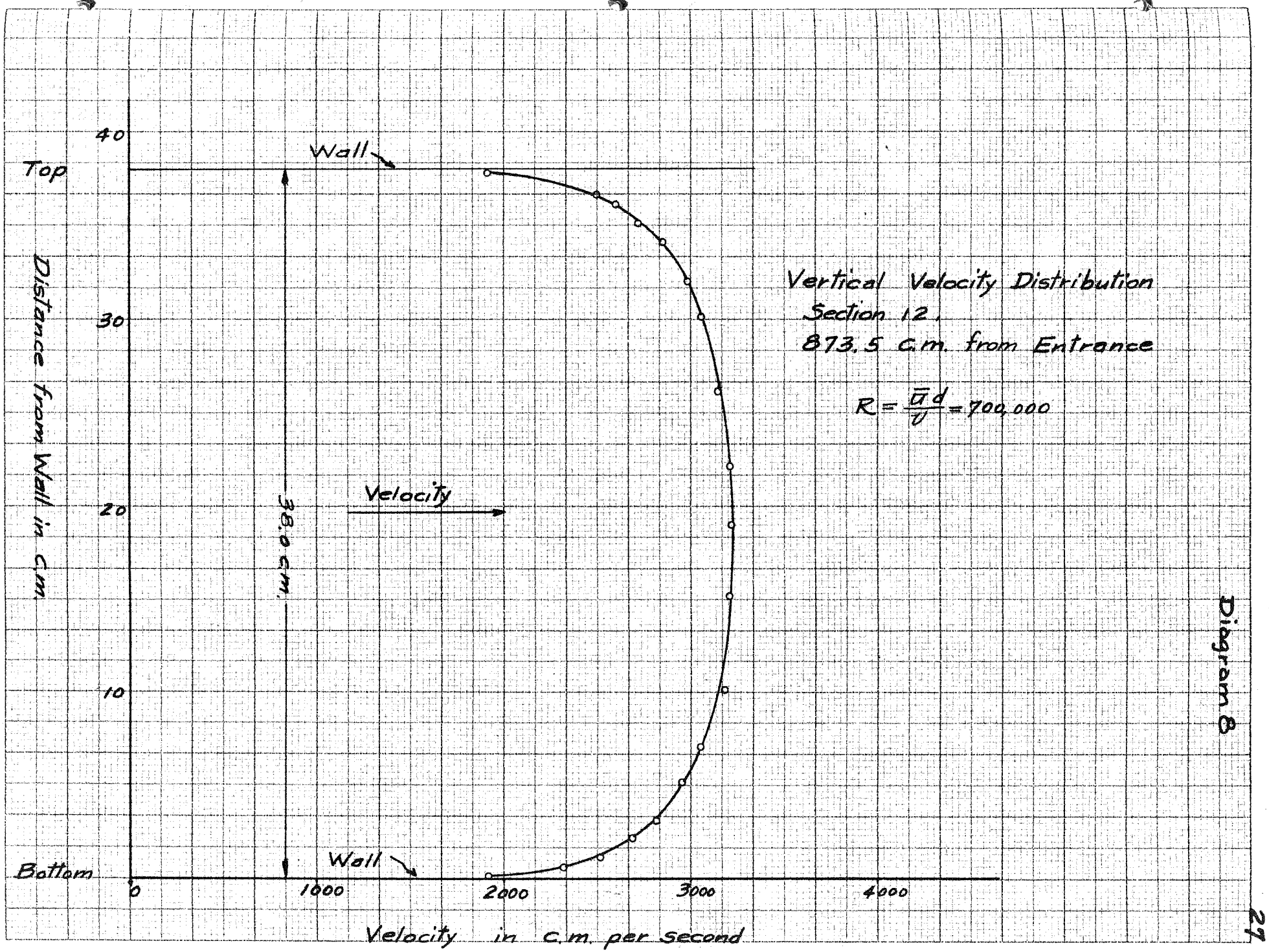
Wall
Top
40
30
20
10
Bottom
Distance from Wall in c.m.
38.0 c.m.
Velocity
Wall
0
1000
2000
3000
4000
Velocity in c.m. per second
Vertical Velocity Distribution
Section 12,
873.5 c.m. from Entrance
$R = \frac{\bar{v} d}{\nu} = 700,000$
Diagram 8

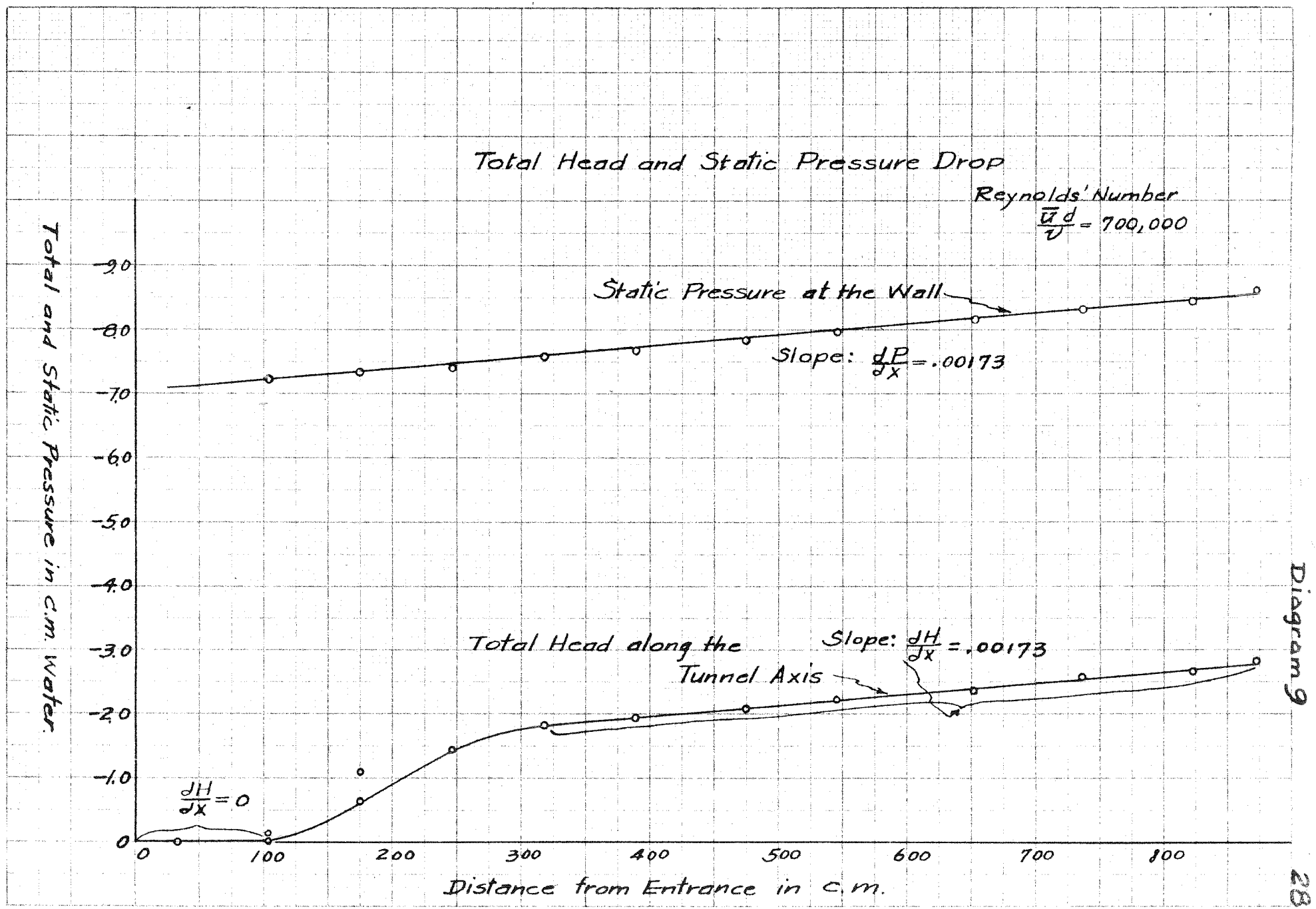
Total Head and Static Pressure Drop
Reynolds' Number
$\frac{\bar{u}d}{\nu}$ = 700,000
Static Pressure at the Wall
Slope: $\frac{dP}{dx}$ = .00173
Total Head along the Tunnel Axis
Slope: $\frac{dH}{dx}$ = .00173
$\frac{dH}{dx}$ = 0
Total and Static Pressure in c.m. Water
Distance from Entrance in c.m.
-9.0
-8.0
-7.0
-6.0
-5.0
-4.0
-3.0
-2.0
-1.0
0
0
100
200
300
400
500
600
700
800

Diagram 9

(1) Near the Wall-----Using the small Pitot tube, the velocity distribution near the wall was measured and the results were plotted on Diags. 6 and 7.

(2) Over the Section ---- Using the large Pitot tube, the velocity distribution across the tunnel was measured and the results were plotted on Diags. 7 and 8.

(3) Total head drop along the central axis of the tunnel at 11 different sections and static pressure drops at the wall at 11 different corresponding sections were measured and the results were plotted on Diag. 9.

In the Diag. 7, the velocity distribution near the wall as well as across the section were plotted on a logarithmic scale. The curve was found to be straight and to have a slope of 1/9.6 or the value of "n" greater than that for a laminar flow. This indicated that the flow was turbulent all the way across the section. In the Diag. 9, we note that the total head drop curve has a zero slope near the entrance, and going through a transitional region at 100-300 cm. from the entrance, it assumes a slope of .00173, which is the same as the slope of the static pressure drop curve above. As the total head drop was measured at the center of the section, before the boundary layers meet, the flow should be potential, because the wall friction does not affect the flow at the center until the boundary layers from the opposite walls meet. If we express a total head drop, in a potential flow,

$$\frac{\partial H}{\partial x} = \frac{\partial}{\partial x}\left(P_{static} + \frac{\rho U^2}{2}\right) = 0$$

where,

H--total head,
x--direction of the tunnel axis,
P--static pressure
U--velocity of the flow
ρ--density of the fluid (air)

The tunnel being parallel and straight, the static pressure drop is a straight line function, as it is affected only by a constant wall friction. When the flow is completely turbulent throughout the section, the velocity of the flow remains constant along the axis and as the density of the air remains sufficiently constant for our purpose,

$$\frac{\partial}{\partial x}\left(\frac{\rho U^2}{2}\right) = 0$$

and we have,

$$\frac{\partial H}{\partial x} = \frac{\partial P_{static}}{\partial x}$$

This means that the completely turbulent flow has the same total head drop along the axis as the static pressure drop at the wall.

Therefore, from the Diags. 6-9 inclusive, we conclude that the flow at the section beyond the point 350 cm. from the entrance is a completely developed turbulent one. The section 12 (873.5 cm. from the entrance) therefore is sufficiently far back to give a fully developed turbulence, when the entrance condition is as shown in the Fig. 14, and when the motor is run at its normal speed.

THEORY OF FULLY DEVELOPED TURBULENCE

Prandtl Theory of Mischungsweg (Ref. 15 and 16)

Boussinesq, in order to determine the mean velocity of a fully developed turbulence, originated a formula which includes an "apparent viscosity" ε in place of μ, the coefficient of viscosity in the equation for the shearing stress,

$$\tau = \rho \varepsilon \left(\frac{d\bar{u}}{dy} \right) \qquad (1)$$

where,

τ ----shearing stress,
ρ ----density of fluid,
ε ----apparent viscosity,
$\bar{u}$ ----velocity (time average)
y----Cartesian coordinate axis perpendicular to the direction of the velocity U.

This formula has the disadvantage that the apparent viscosity itself depends in turn on the velocity which must therefore first be found. Therefore, it has been found convenient to divide the instantaneous velocity into two components, the time mean value and the oscillation about this value,

$$u = \bar{u} + u' \qquad v = \bar{v} + v' \qquad w = \bar{w} + w'$$

In the average the oscillations now give an apparent state of shear whose components are constructed from the momentum components,

$$\tau_{xx} = -\overline{\rho u'^2} \qquad \tau_{xy} = -\overline{\rho u' v'} \qquad \tau_{yy} = -\overline{\rho v'^2} \quad \text{etc.}$$

The bar over the quantities denotes time average values.

In a turbulent flow, it is the shearing stress that has the greatest influence upon the motion. Prandtl therefore proceeded to evaluate τ_{xy} in terms of the mean flow velocities

$\bar{u}$, $\bar{v}$ and a quantity which he introduced and called l ="mischungsweg". This length is in some ways analoguous to the idea of the mean free path in the kinetic theory.

Prandtl then considered the flow in the x direction, so that $\bar{u}$ is a function of y alone. A particle of fluid is displaced through a distance l from one layer to another. If the particle had initially the mean speed of the first layer, then , upon displacement, it will have a difference of speed from its neighbouring particle by an amount $l \frac{d\bar{u}}{dy}$ to a first approximation. Modifying l to represent the mean distance across the main flow travelled by particles from the first layer before they lose their initial character, then it is seen that the mean oscillation at the point is

$$u' = l \left(\frac{d\bar{u}}{dy}\right)$$

Regarding the oscillation v' as being induced by the motion of particles having opposite values of u', then the mean v' can be set proportional to the mean u'. For the apparent stress it may now be written:

$$\tau_{xy} = \rho l^2 \left|\frac{d\bar{u}}{dy}\right| \cdot \frac{d\bar{u}}{dy} \qquad (2)$$

where the form assumed allows for change of sign of τ_{xy} with change of sign of $\frac{d\bar{u}}{dy}$. It has to be noted that l is considered to contain any necessary numerical coefficients, such that equality instead of proportionality between the quantities may be used.

Unlike ν , the kinematic coefficient of viscosity in the formula of shearing stress for laminar flow,

$$\tau = \mu \left(\frac{du}{dy}\right) = \rho \nu \left(\frac{du}{dy}\right)$$

ε the apparent viscosity in the expression for the shearing stress of turbulent flow $\tau = \rho\varepsilon\left(\frac{d\bar{u}}{dy}\right)$ will vary from place to place in the fluid, and will also be a function of the velocity. A comparison of (1) and (2) shows that we can express

$$\varepsilon = l^2 \left|\frac{d\bar{u}}{dy}\right| \tag{3}$$

This gives,

$$\tau = \rho l^2 \left(\frac{d\bar{u}}{dy}\right)^2$$

and mischungsweg,

$$l = \frac{\sqrt{\frac{\tau}{\rho}}}{\left(\frac{d\bar{u}}{dy}\right)} \tag{4}$$

This relation is not accurate enough under certain circumstances, especially near the center of the channel, and hence a second approximation for ε has to be found. Instead of taking $\left|\frac{d\bar{u}}{dy}\right|$, it would be more accurate to consider its statistical average over the section of breadth $2l$ vis. $\overline{\left\{\left(\frac{du}{dy}\right)^2\right\}}^{\frac{1}{2}}$, which by development in a Taylor series, can be expressed in the approximate form

$$\left\{\left(\frac{d\bar{u}}{dy}\right)^2 + l'^2\left(\frac{d^2\bar{u}}{dy^2}\right)^2\right\}^{\frac{1}{2}}$$

Therefore, the more accurate expression is

$$\varepsilon = l^2\left\{\left(\frac{d\bar{u}}{dy}\right)^2 + l'^2\left(\frac{d^2\bar{u}}{dy^2}\right)^2\right\}^{\frac{1}{2}} \tag{5}$$

This varies little from (3) when $d\bar{u}/dy$ is great, and remains valid where the velocity gradient approaches zero. In the above equation, the value of l' may be determined in the following manner. The previously determined curve for l is extrapolated to the center, assuming in this region that,

$$l = \text{constant} = l_o \qquad \text{(say)}$$

In the same way, near the center we assume,

$$\varepsilon = \text{constant} = \varepsilon_o \qquad \text{(say)}$$

Then (5) becomes,

$$l_o^2 = \frac{\varepsilon_o}{l'^2 \left(\frac{d^2\bar{u}}{dy^2}\right)^2} \qquad (6)$$

From this, l' is calculated. Substituting the value of this l' in (5) a second approximation for l is then calculated for the neighborhood of the center of the channel.

Shearing Stress in the Turbulent Flow

Since in a fully developed turbulent flow, the flow condition does not change from section to section, the exact equillibrium condition reduces to:

$$\pi y^2 \frac{dp}{dx} = 2\pi y \tau \qquad (7)$$

where,
dp/dx ----pressure drop per unit length
=constant.
y-----distance from the axis of the channel,
τ-----shearing stress in the fluid.

Then

$$\tau = \text{constant} \cdot y \qquad (8)$$

Now, the shearing stress at the wall, by similar reasoning,

$$\pi r^2 \frac{dp}{dx} = 2\pi r \tau_o$$

where,
τ_o ---shearing stress at the wall, (or wall friction)
r-----radius of the channel.

Reducing we obtain a relation between the wall friction and the pressure drop,

$$\tau_o = \frac{dP}{dx}\frac{r}{2} \qquad (9)$$

Since dP/dx is constant for a fully developed turbulent flow in a parallel channel,

$$\tau_o = c \cdot r \qquad \text{where, } c\text{---constant}$$

Combining the above expression and (8) we obtain,

$$\tau = \tau_o \frac{y}{r} \qquad (10)$$

Kármán Formula for Mischungsweg Distribution

Kármán has given an interesting interpretation of mischungsweg (Ref. 13). He investigated the conditions to be satisfied for mechanical similarity of the fluctuating motions at two points in the fluid. It is assumed that the main flow is parallel to the x-direction and that the fluctuating flow consists of disturbances confined mainly to the direction of the mean flow. The mean speed of a 2 dimensional flow relative to a definite layer may be expressed as, (origin at the center of the sheet element under consideration)

$$\bar{U} = \bar{u}_o' y + \bar{u}_o'' \frac{y^2}{2} + \bar{u}_o''' \frac{y^3}{3} + \cdots\cdots\cdots$$

Then the stream function for the complete flow near to this layer and relative to it may be taken as

$$\psi(x, y) = \bar{u}_o' \frac{y^2}{2} + \bar{u}_o' \frac{y^3}{6} + \cdots\cdots + \psi_1(x,y)$$

where $\psi_1(x, y)$ is the stream function of the oscillatory motion.

The vibrational motion is regarded at least during a definite interval of time, as a stationary flow superimposed upon the main flow. The hydrodynamic equations for plane steady flow may be combined in the so-called vortex transfer equation,

$$\frac{\partial \psi}{\partial y}\frac{\partial \Delta\psi}{\partial x} - \frac{\partial \psi}{\partial x}\frac{\partial \Delta\psi}{\partial y} = \nu \Delta\Delta\psi$$

where,

$$\Delta\psi = \frac{\partial^2\psi}{\partial x^2} + \frac{\partial^2\psi}{\partial y^2}$$

$\Delta\psi$ is the vortex intensity and ν the kinematic viscosity. Disregarding the friction terms and limiting ourselves, in accordance with the assumed definition of the field of oscillation in the vicinity of axis $y = 0$ to the first approximation neglecting higher order terms than the first,

$$\left(\bar{u}_o' y + \frac{\partial \psi}{\partial y}\right)\frac{\partial \Delta\psi}{\partial x} - \frac{\partial \psi}{\partial x}\bar{u}_o'' - \frac{\partial \psi}{\partial x}\frac{\partial \Delta\psi}{\partial y} = 0$$

Transforming the above equation by means of the substitution

$$x = l\xi \qquad y = l\eta \qquad \psi_1 = A\, f(\xi, \eta)$$

it becomes:

$$\left\{\bar{u}_o' l\eta + \frac{A}{l}\frac{\partial f}{\partial \eta}\right\}\frac{A}{l^3}\frac{\partial \Delta f}{\partial \xi} - \frac{A}{l}\frac{\partial f}{\partial \xi}\left\{\bar{u}_o'' + \frac{A}{l^3}\frac{\partial \Delta f}{\partial \eta}\right\} = 0$$

where the operator Δ applies to the variables ξ, η

The quantities l and A are functions of position, that is functions of $\bar{u}_o'$, $\bar{u}_o''$ etc., whereas $f(\xi, \eta)$ is to be independent of these variables, according to Kármán's definition of similarity. Thus, the above equation will be satisfied independently of l and A (i.e. of $\bar{u}_o'$, $\bar{u}_o''$ etc.) when,

a) $\bar{u}_o' \, l$ is proportional to $\frac{A}{l}$

b) $\bar{u}_o''$ is proportional to $\frac{A}{l^3}$

Hence l and A must be proportional to $\frac{\bar{u}_o'}{\bar{u}_o''} = \frac{\frac{\partial \bar{u}}{\partial y}}{\frac{\partial^2 \bar{u}}{\partial y^2}}$ and $\frac{\bar{u}_o'^3}{\bar{u}_o''^2}$ (or $l^2 \bar{u}_o'$) respectively.

Consider now the shearing stress due to turbulence. This is

$$\tau = -\overline{\rho u'v'} = \rho \frac{\partial \psi}{\partial x} \cdot \frac{\partial \psi_1}{\partial y}$$

$$= \rho \frac{A^2}{l^2} \frac{\partial f}{\partial \xi} \frac{\partial f}{\partial \eta} = \kappa^2 \rho \frac{\bar{u}_o'^4}{\bar{u}_o''^2}$$

The Prandtl expression, as given previously is $\tau = \rho l^2 \bar{u}_o'^2$. A comparison of the two expressions shows that the mischungsweg may be expressed as:

$$l = \kappa \frac{\frac{\partial u}{\partial y}}{\frac{\partial^2 u}{\partial y^2}} = \kappa \frac{\bar{u}_o'}{\bar{u}_o''} \qquad (11)$$

where,

k---non-dimensional constant universal for all turbulent flows, depending only upon the nature of the fluctuations, i.e. upon the solution of the equation

for $f(\xi, \eta)$.

According to the measurements of Dönch and Nikuradse, the value of k appears to be $k = .36$, while the resistance law gives according to Kármán (Ref. 13) $k = .38$. Therefore, according to the Kármán formula, the mischungsweg is k times the quotient of the first and the second derivatives of the velocity distribution curve of the mean flow.

Von Kármán (Ref. 13) reduced the formula (11) and

obtained,

$$l = \kappa \frac{\bar{u}'}{\bar{u}''} = 2\kappa h \sqrt{\frac{y}{h}} \left(1 - \sqrt{\frac{y}{h}}\right)$$

Since near the wall,

$$y = h - y_1$$

where, $h = \frac{1}{2}$ width of the channel.

mischungsweg becomes,

$$l = 2\kappa h \left\{ \sqrt{1 - \frac{y_1}{h}} + \frac{y_1}{h} - 1 \right\} \qquad (12)$$

$$l = \kappa y_1 \left(1 - \frac{y_1}{4h} - \frac{y_1^2}{8h} - \ldots\ldots\ldots\ldots\right)$$

This formula was developed to hold for 2-dimensional flow in a channel but immediately near the wall it may be used in our case of a three dimensional flow.

The Power Law

It is known that the resistance law within a large range of Reynolds Numbers can be expressed by the interpolation formula, (Ref. 20 and 24),

$$\log(\lambda) = -m \log(R)$$

R --Reynolds Number
λ-- resistance coef.

$$\lambda = \frac{\text{constant}}{R^m}$$

Upon this premise, it can be proven by a line of reasoning advanced by Prandtl and Kármán that the velocity distribution is given by formula,

$$u = \text{constant} \sqrt{\frac{\tau_o}{\rho}} \left(\frac{\sqrt{\frac{\tau_o}{\rho}}}{\nu} y \right)^{\frac{m}{2-m}}$$

Except in the immediate neighborhood of the wall and near the center of the channel, this formula is valid.

Putting,

$$\frac{m}{2 - m} = \frac{1}{n}$$

we have,

$$U = c\sqrt{\frac{\tau_o}{\rho}}\left(\frac{\sqrt{\frac{\tau_o}{\rho}}}{\nu} y\right)^{\frac{1}{n}}$$

$$U = \text{constant} \cdot y^{\frac{1}{n}} \qquad (13)$$

for a given flow.

The exponent n increases as Reynolds Number increases.

Diagram 10

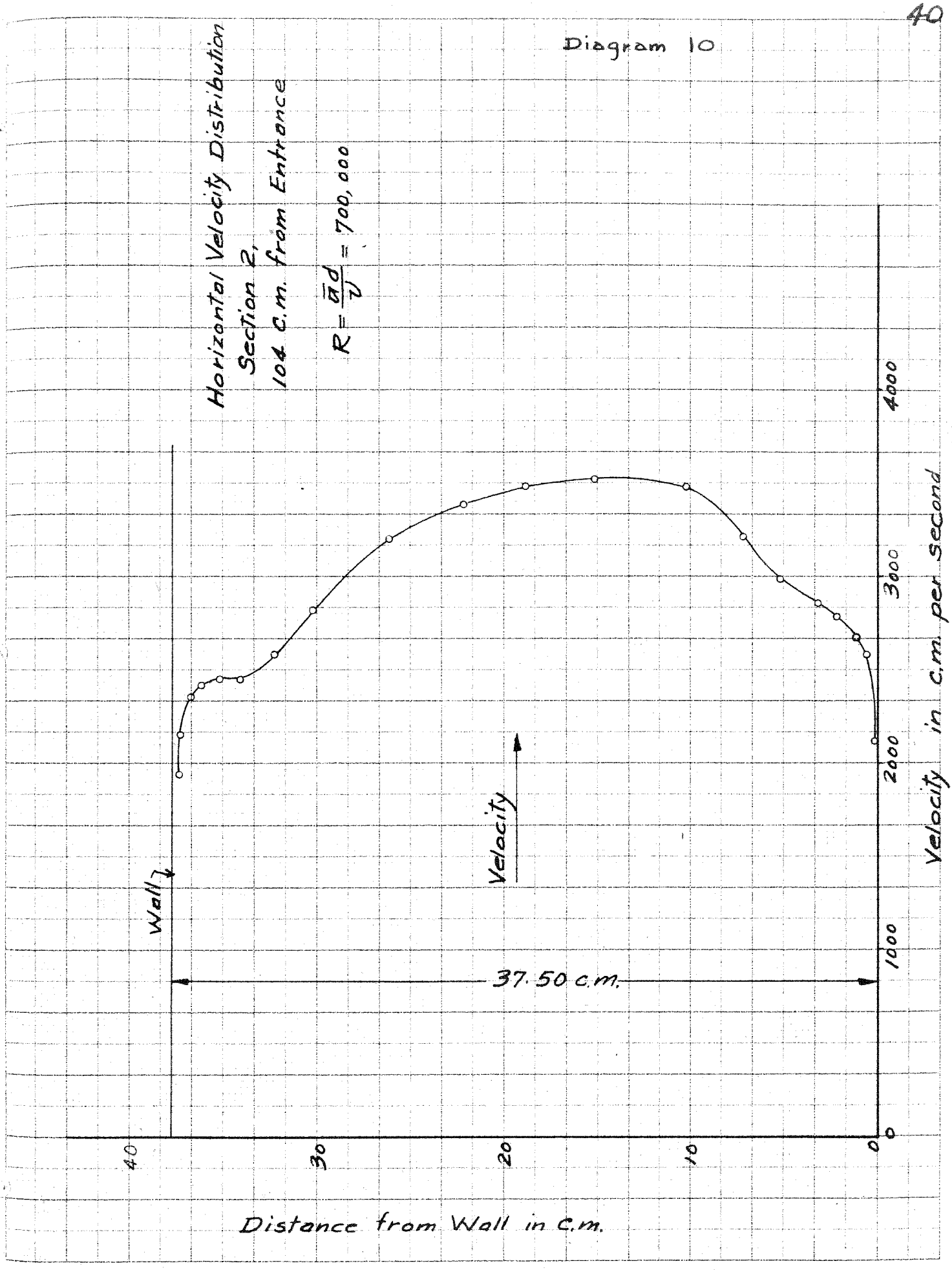
Horizontal Velocity Distribution
Section 2,
104 c.m. from Entrance
$R = \frac{\bar{a} d}{\nu} = 700,000$
Wall
Velocity
37.50 c.m.
0
1000
2000
3000
4000
Velocity in c.m. per second
40
30
20
10
0
Distance from Wall in c.m.

Diagram 11

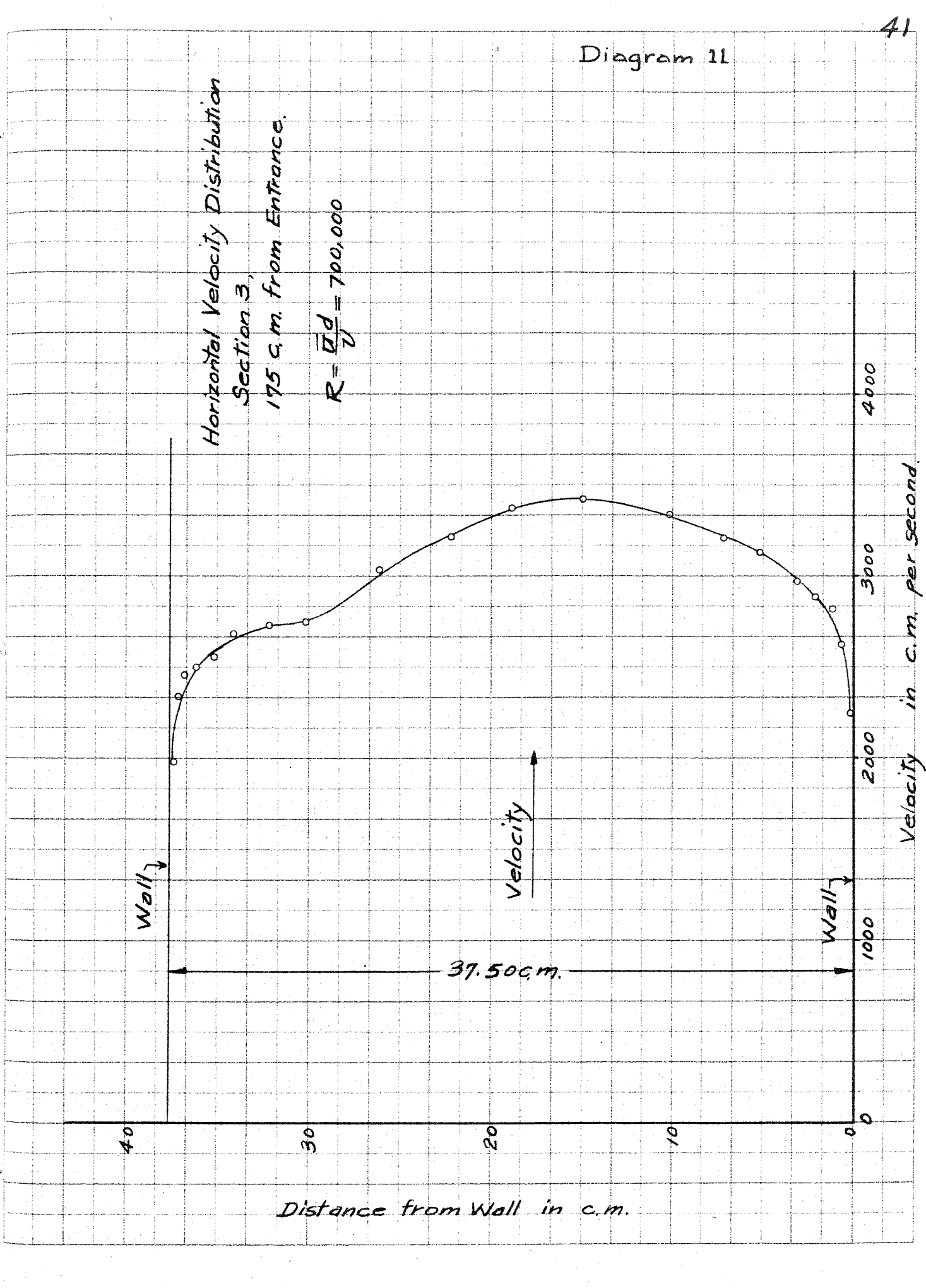
Horizontal Velocity Distribution
Section 3,
175 c.m. from Entrance.
$R = \frac{\bar{v} d}{\nu} = 700,000$
Wall
Velocity
Wall
37.50 c.m.
0
1000
2000
3000
4000
Velocity in c.m. per second.
40
30
20
10
0
Distance from Wall in c.m.

Diagram 12

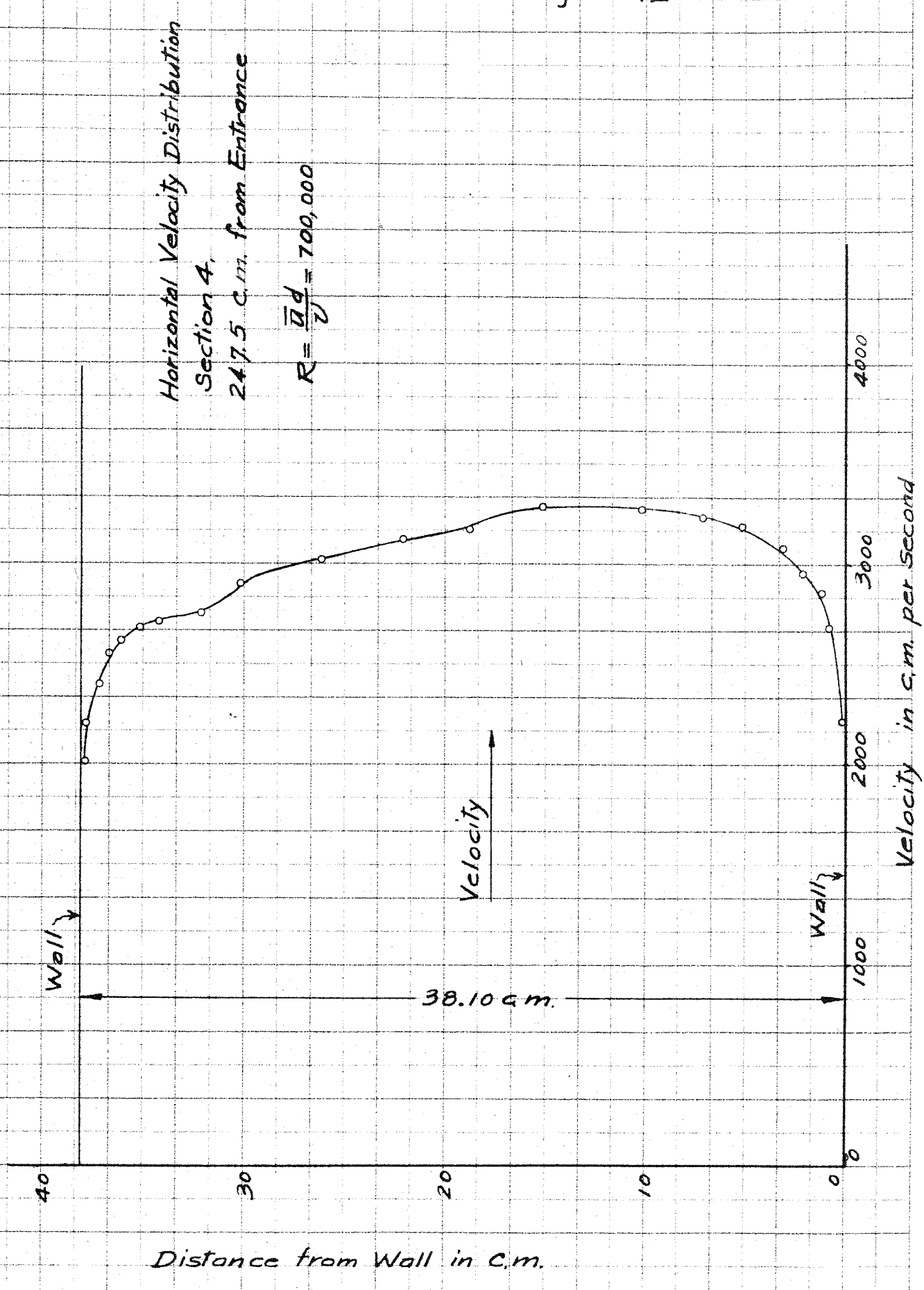
Horizontal Velocity Distribution
Section 4,
247.5 c.m. from Entrance
$R = \frac{\overline{v}\,d}{\nu} = 700,000$
Velocity
Wall
Wall
38.10 c.m.
Velocity in c.m. per Second
0
1000
2000
3000
4000
40
30
20
10
0
Distance from Wall in c.m.

Diagram 13.

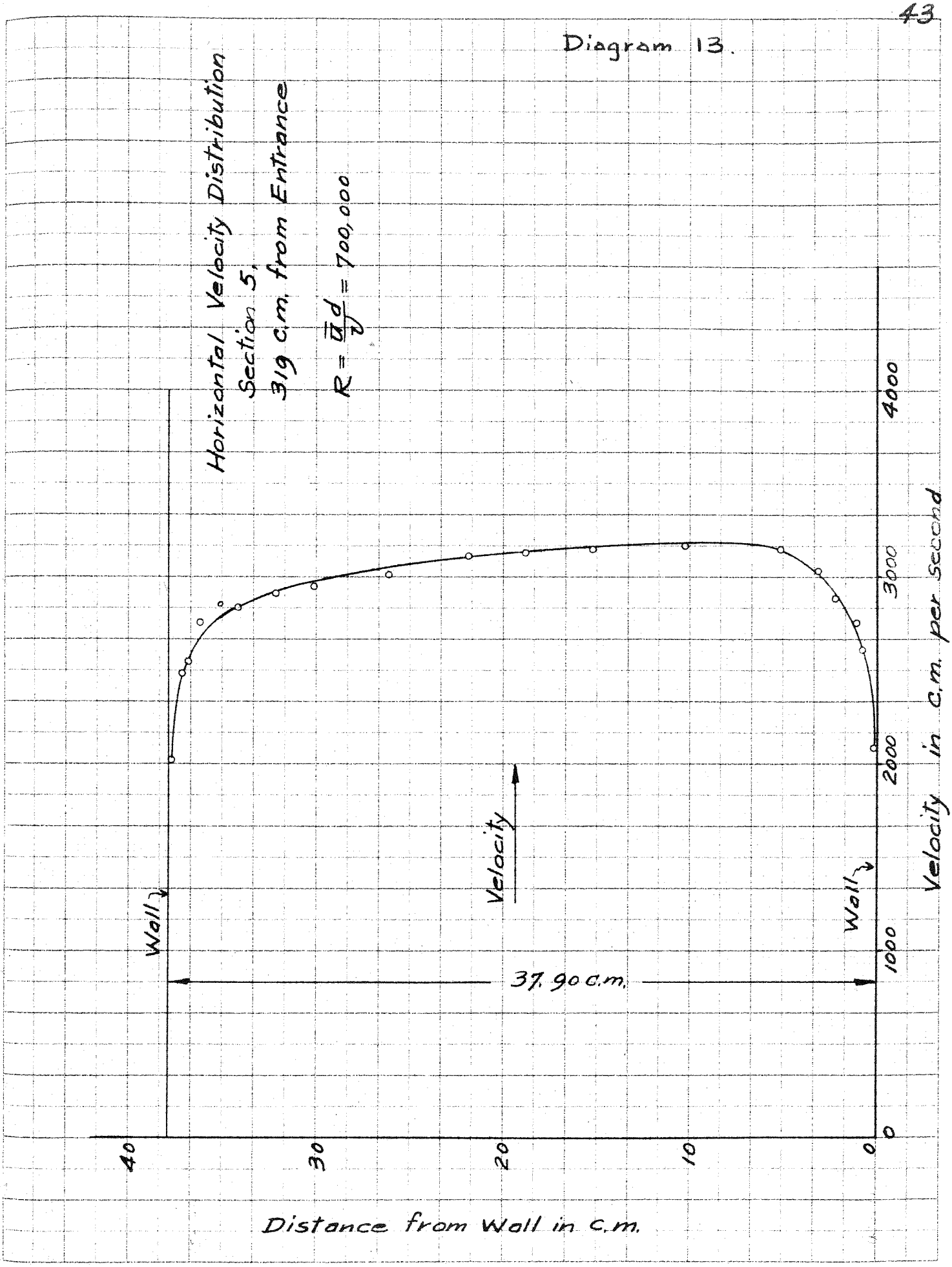
Horizontal Velocity Distribution
Section 5,
319 c.m. from Entrance
$R = \frac{\overline{v}d}{\nu} = 700,000$
Velocity in c.m. per second
4000
3000
2000
1000
0
Wall
Velocity
Wall
37.90 c.m.
40
30
20
10
0
Distance from Wall in c.m.

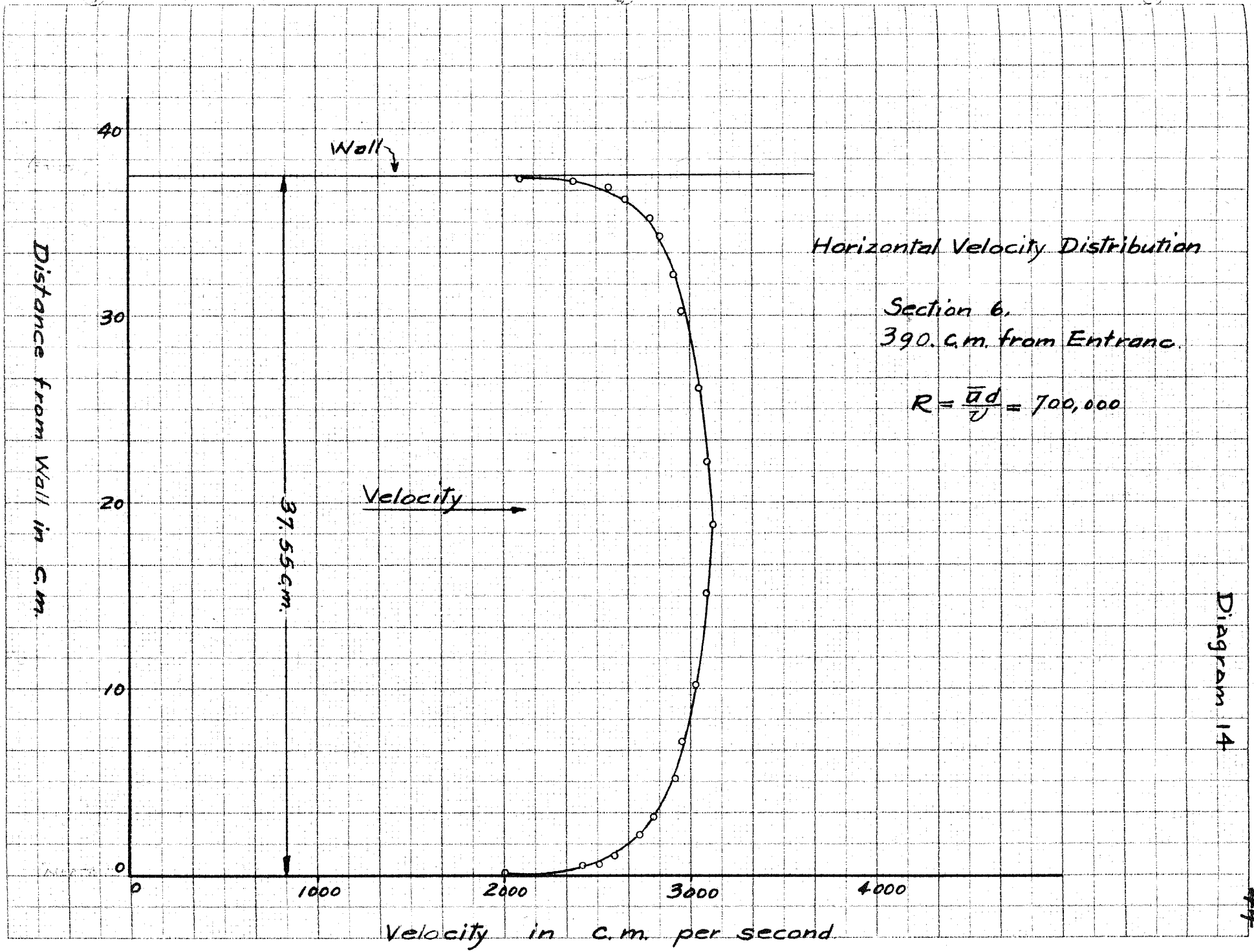

Horizontal Velocity Distribution

Section 6.
390. c.m. from Entranc.

$R = \frac{\bar{u} d}{\nu} = 700,000$

Diagram 14

Diagram 15

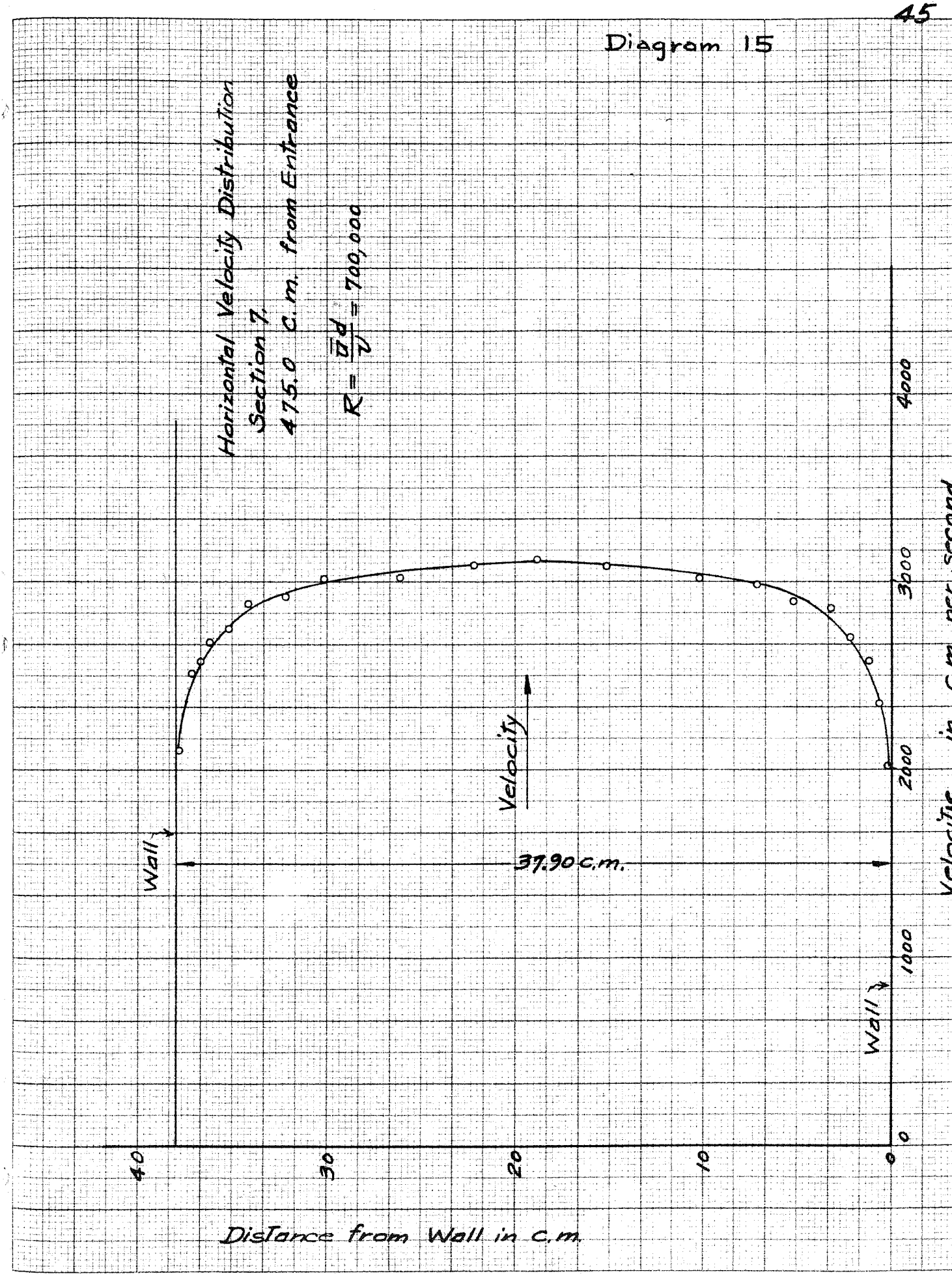
Horizontal Velocity Distribution
Section 7.
475.0 c.m. from Entrance
$R = \frac{\overline{v}d}{\nu} = 700,000$
Velocity
37.90 c.m.
Wall
Wall
0
1000
2000
3000
4000
Velocity in c.m. per second
0
10
20
30
40
Distance from Wall in c.m.

Diagram 16

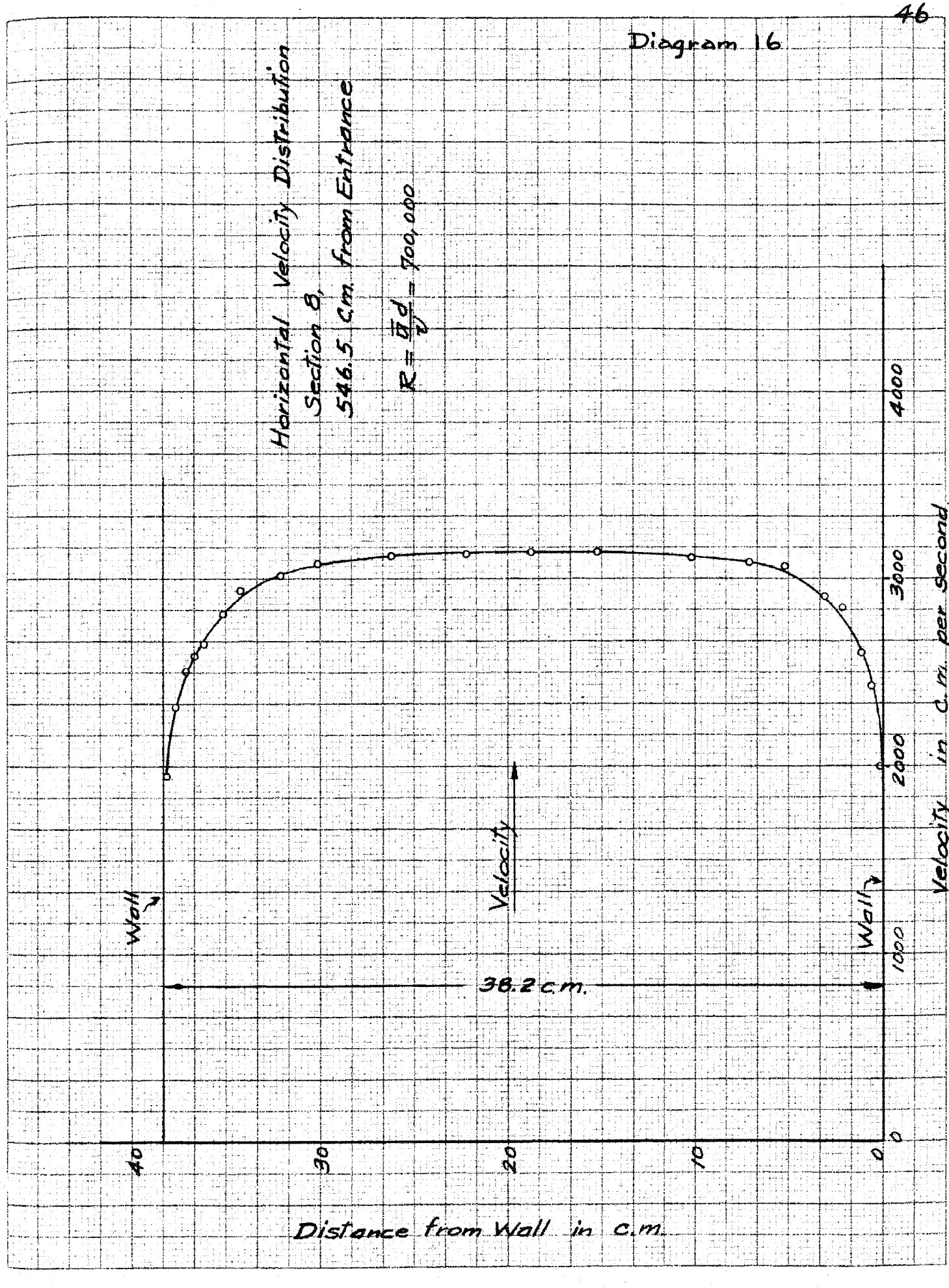
Horizontal Velocity Distribution
Section 8,
546.5 cm. from Entrance
$R = \frac{\overline{v}\, d}{\nu} = 700,000$
Velocity
Wall
38.2 cm.
Wall
0
1000
2000
3000
4000
Velocity in c.m. per second
40
30
20
10
0
Distance from Wall in c.m.

Diagram 17

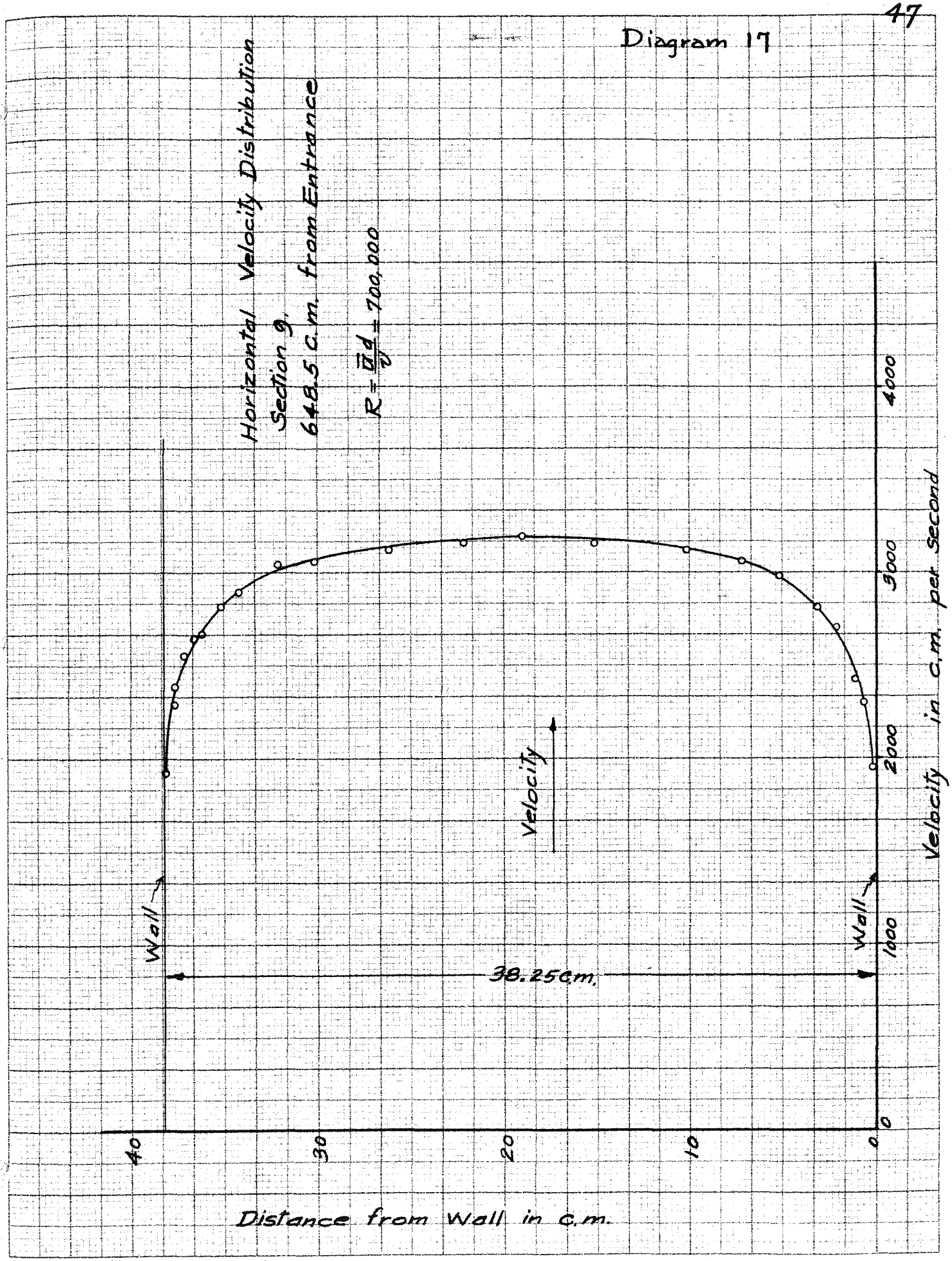
Horizontal Velocity Distribution
Section 9.
648.5 c.m. from Entrance
$R = \frac{\overline{v}d}{\nu} = 700,000$
Velocity
Wall
Wall
38.25 c.m.
Velocity in c.m. per second
0
1000
2000
3000
4000
40
30
20
10
0
Distance from Wall in c.m.

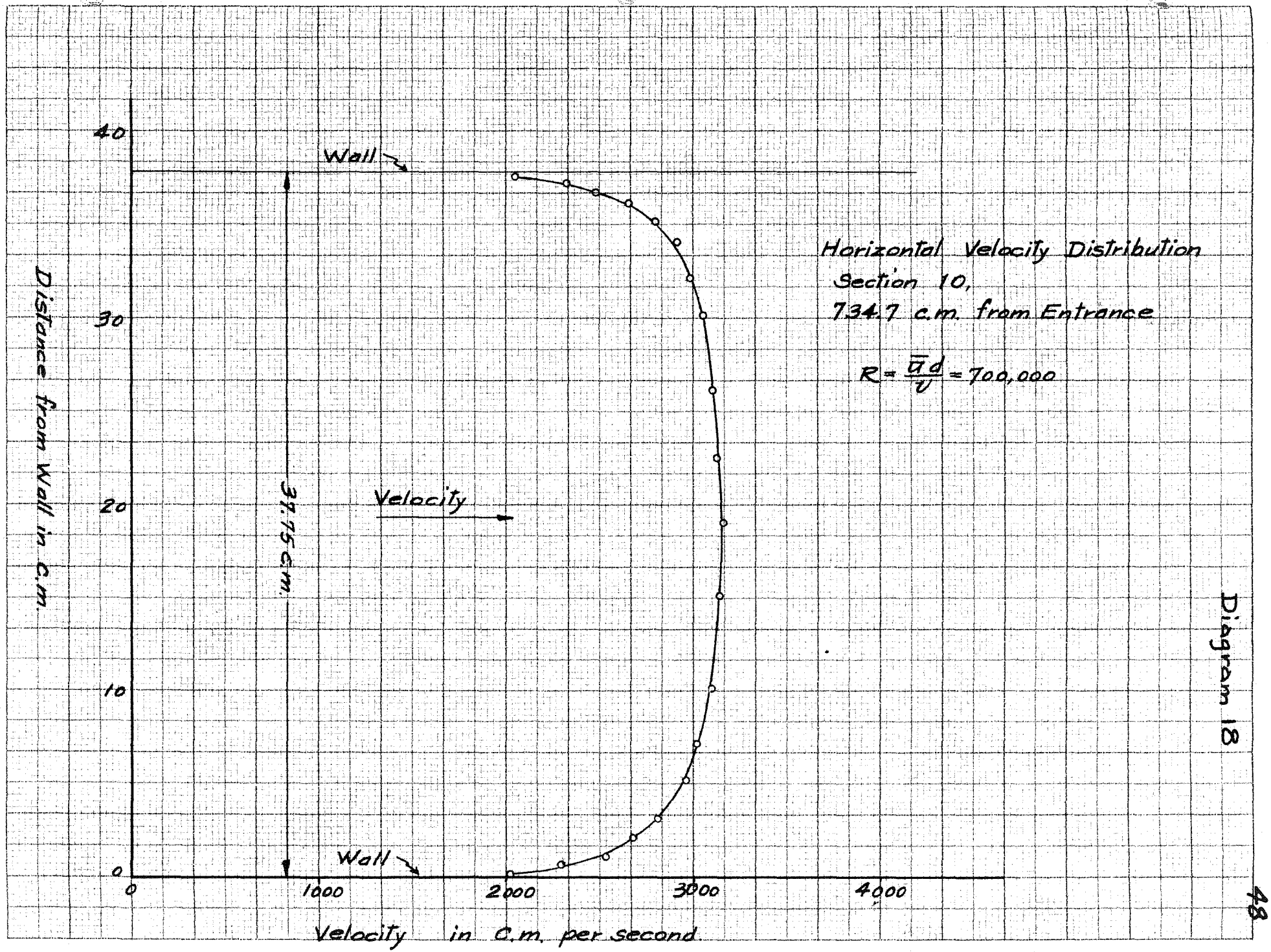
Horizontal Velocity Distribution
Section 10,
734.7 c.m. from Entrance
$R = \frac{\bar{u} d}{\nu} = 700,000$
Wall
Wall
Velocity
37.75 c.m.
Distance from Wall in c.m.
Velocity in c.m. per second
0
10
20
30
40
1000
2000
3000
4000

Diagram 18

Diagram 19.

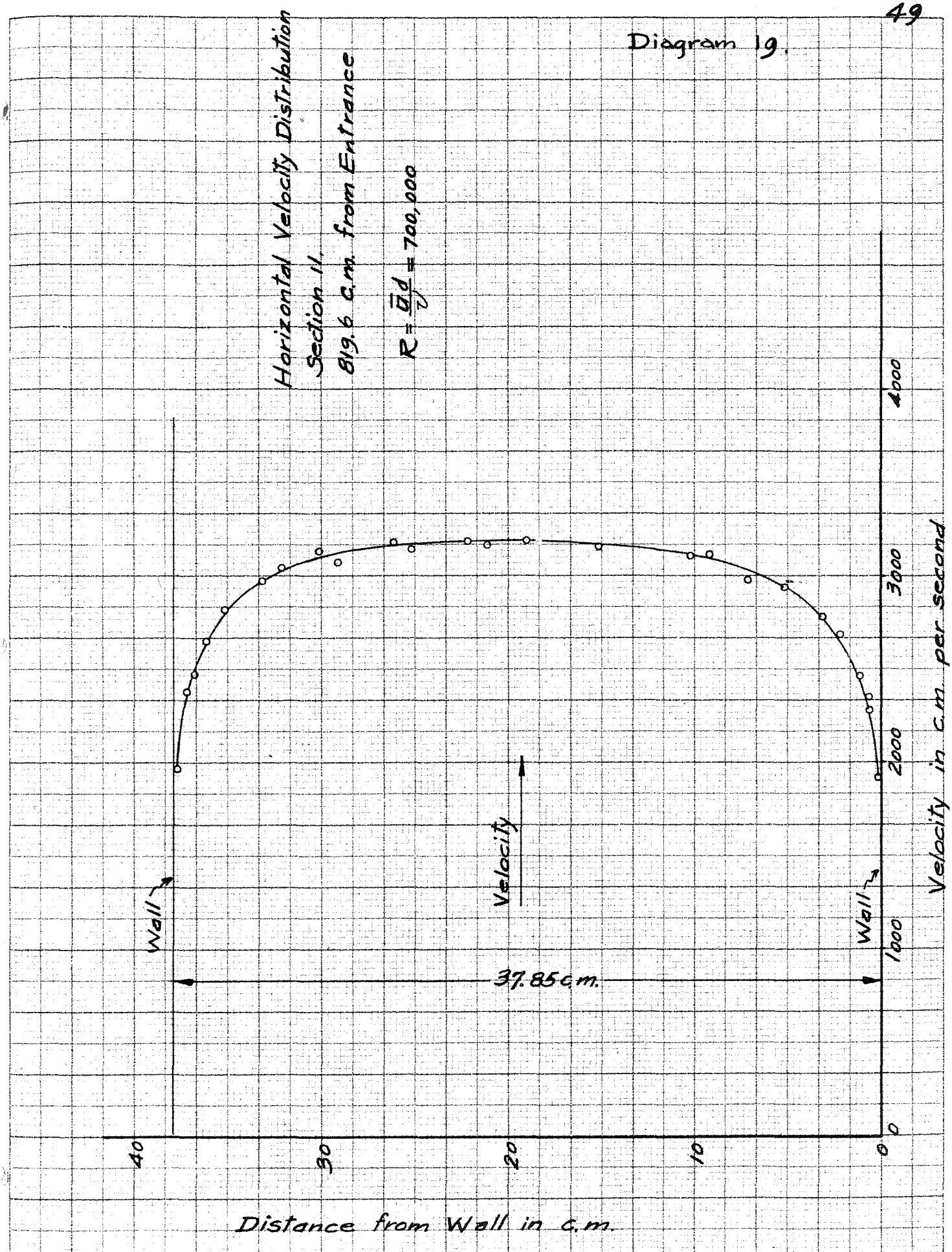
Horizontal Velocity Distribution
Section 11,
819.6 c.m. from Entrance
$R = \frac{\bar{v}d}{\nu} = 700,000$
Velocity
Wall
Wall
37.85 c.m.
Velocity in c.m. per second
0
1000
2000
3000
4000
40
30
20
10
0
Distance from Wall in c.m.

Diagram 20

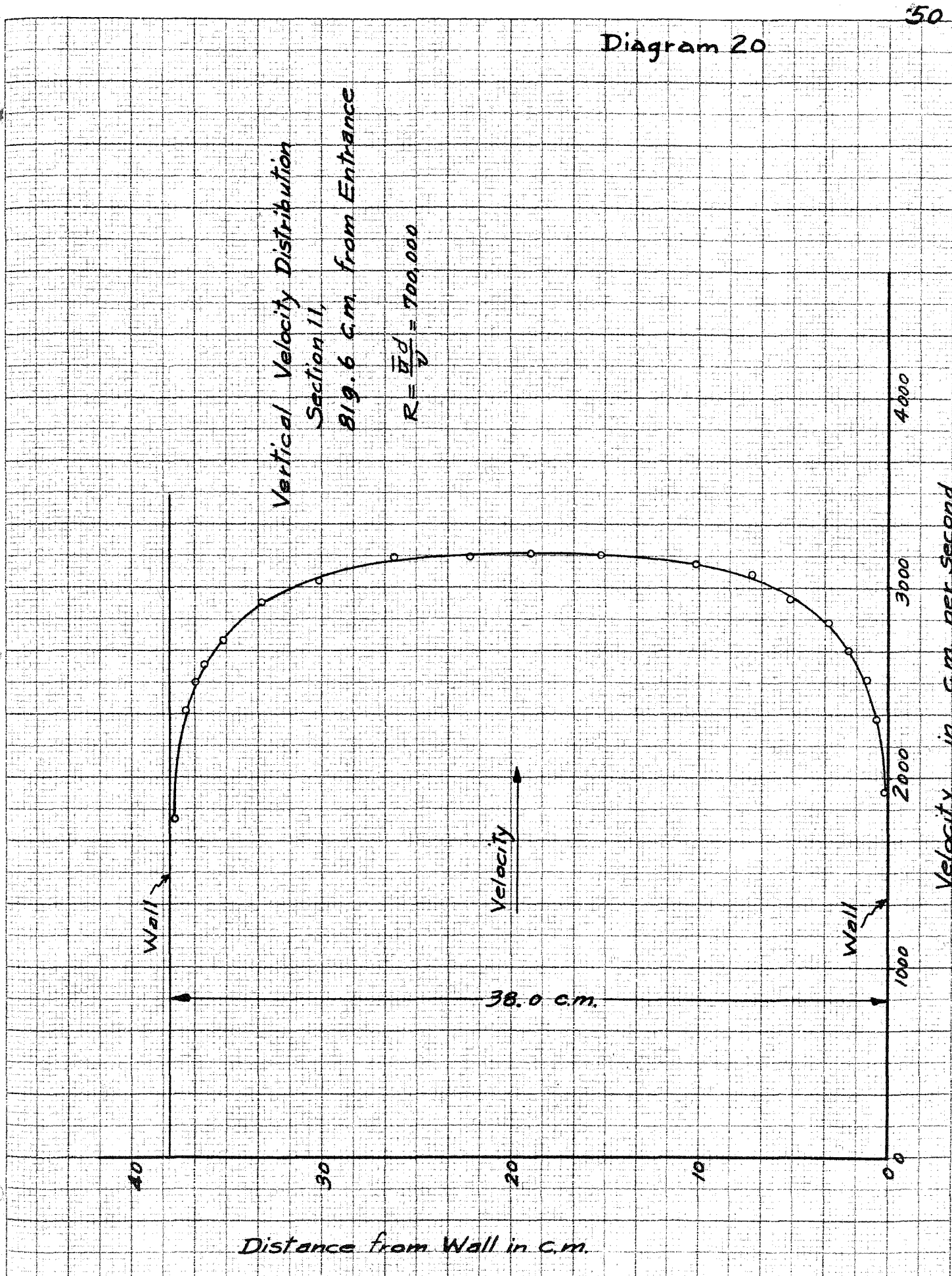
Vertical Velocity Distribution
Section II,
819.6 c.m. from Entrance
$R = \frac{Vd}{\nu} = 700,000$
Wall
Velocity
38.0 c.m.
Wall
0
1000
2000
3000
4000
Velocity in c.m. per second
40
30
20
10
0
Distance from Wall in c.m.

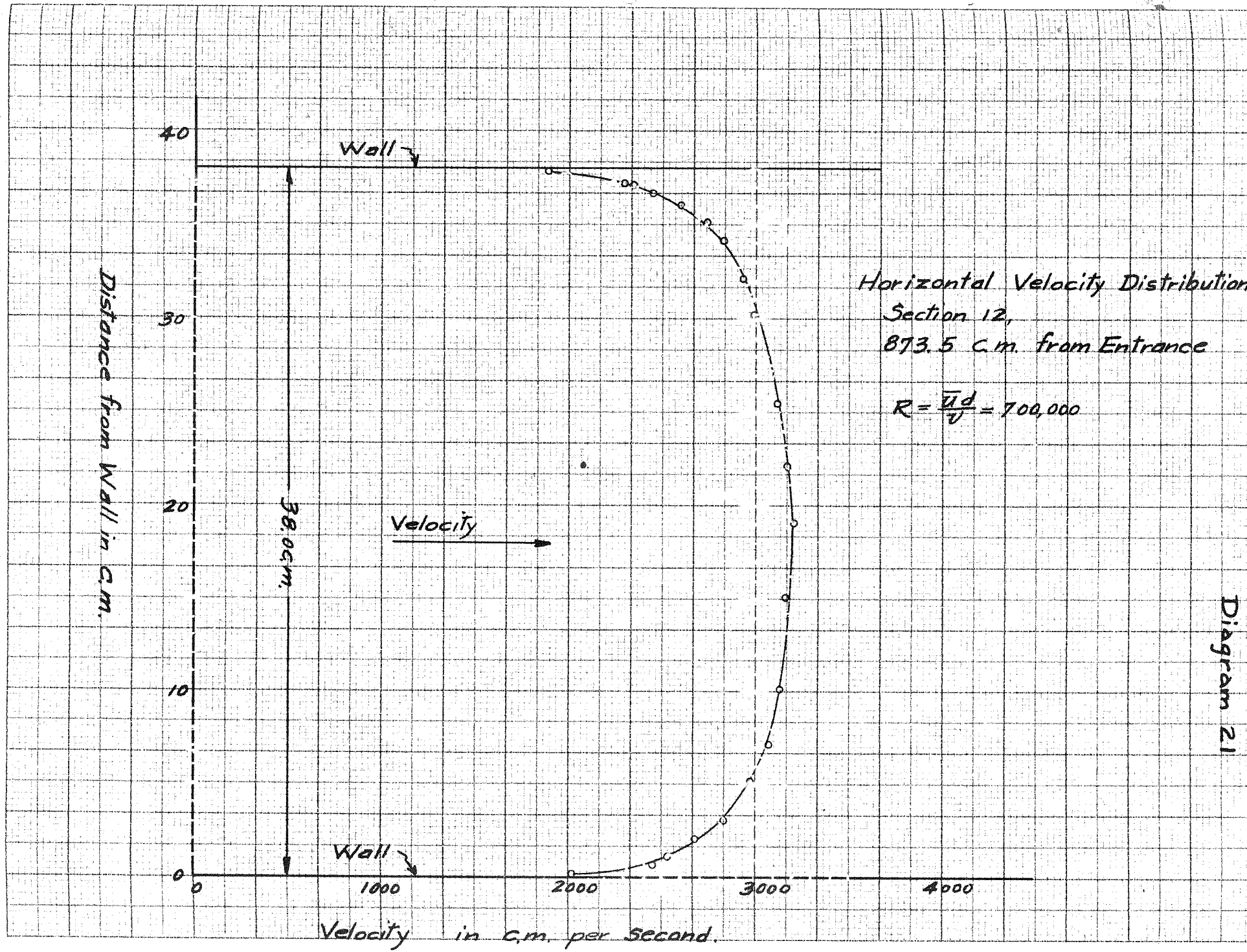
Horizontal Velocity Distribution
Section 12,
873.5 c.m. from Entrance
$R = \frac{\bar{u}d}{\nu} = 700,000$
Diagram 21
Distance from Wall in c.m.
40
30
20
10
0
Wall
38.0 c.m.
Velocity
Wall
0
1000
2000
3000
4000
Velocity in c.m. per Second.

OPPOSITE SIDE

NON-DIMENSIONAL
VELOCITY DISTRIBUTION CURVES.

REYNOLDS' NUMBER: $\frac{\bar{u}D}{\nu} = 700{,}000$

H.-- HORIZONTAL VELOCITY DISTRIBUTION

V.-- VERTICAL VELOCITY DISTRIBUTION

VELOCITY →

DISTANCE FROM WALL / DIAMETER OF TUNNEL $= \frac{y}{D}$

1.00 .90 .80 .70 .60 .50 .40 .30 .20 .10 0

H. 2.74 D. H. 4.61 D. H. 6.5 D. H. 8.93 D. H. 10.27 D. H. 12.5 D. H. 14.38 D. H. 17.07 D. H. 19.32 D. H. 21.57 D. H. 23 D. V. 21.57 D. V. 23.0 D.

2.74 D. 4.61 D. 6.5 D. 8.93 D. 10.27 D. 12.5 D. 14.38 D. 17.07 D. 19.32 D. 21.57 D. 23.0 D. V. 21.57 D. V. 23.0 D.

0 .1 .2 .3 .4 .5 .6 .7 .8 .9 1.0 1.1

LOCAL VELOCITY / MEAN VELOCITY $= \frac{u}{\bar{u}}$ →

O POINT FOR SECTION 2.74 DIAMETERS FROM ENTRANCE. VELOCITY DISTRIBUTION AT

Diagram 23

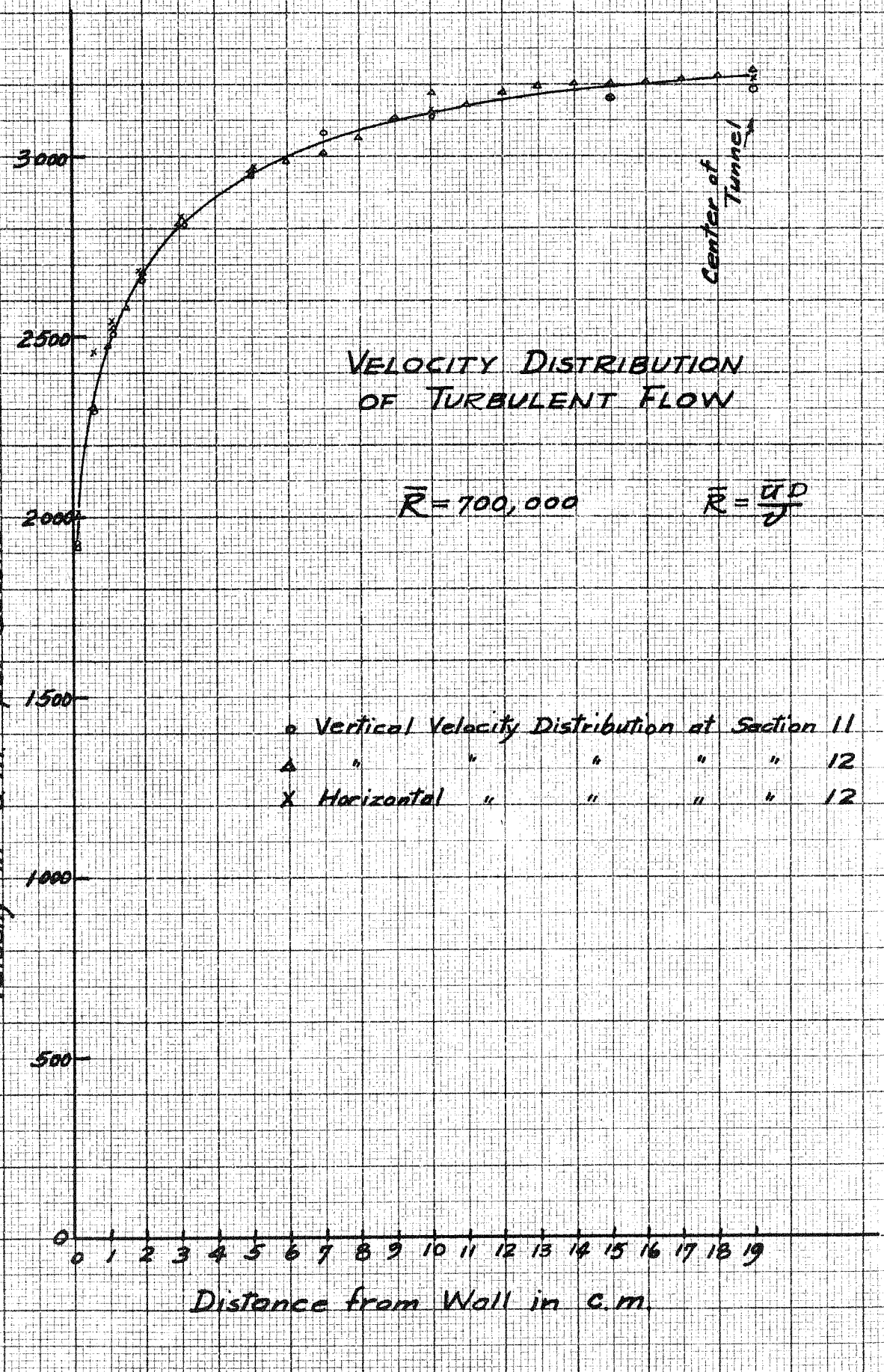

VELOCITY DISTRIBUTION OF TURBULENT FLOW

$\bar{R} = 700,000$ $\qquad \bar{R} = \frac{\bar{U} D}{\nu}$

o Vertical Velocity Distribution at Section 11

Δ " " " " " 12

X Horizontal " " " " 12

Diagram 24

Dimensionless Velocity Distribution of Turbulent Flow

$$R = \frac{\bar{U} D}{\nu} = 700{,}000$$

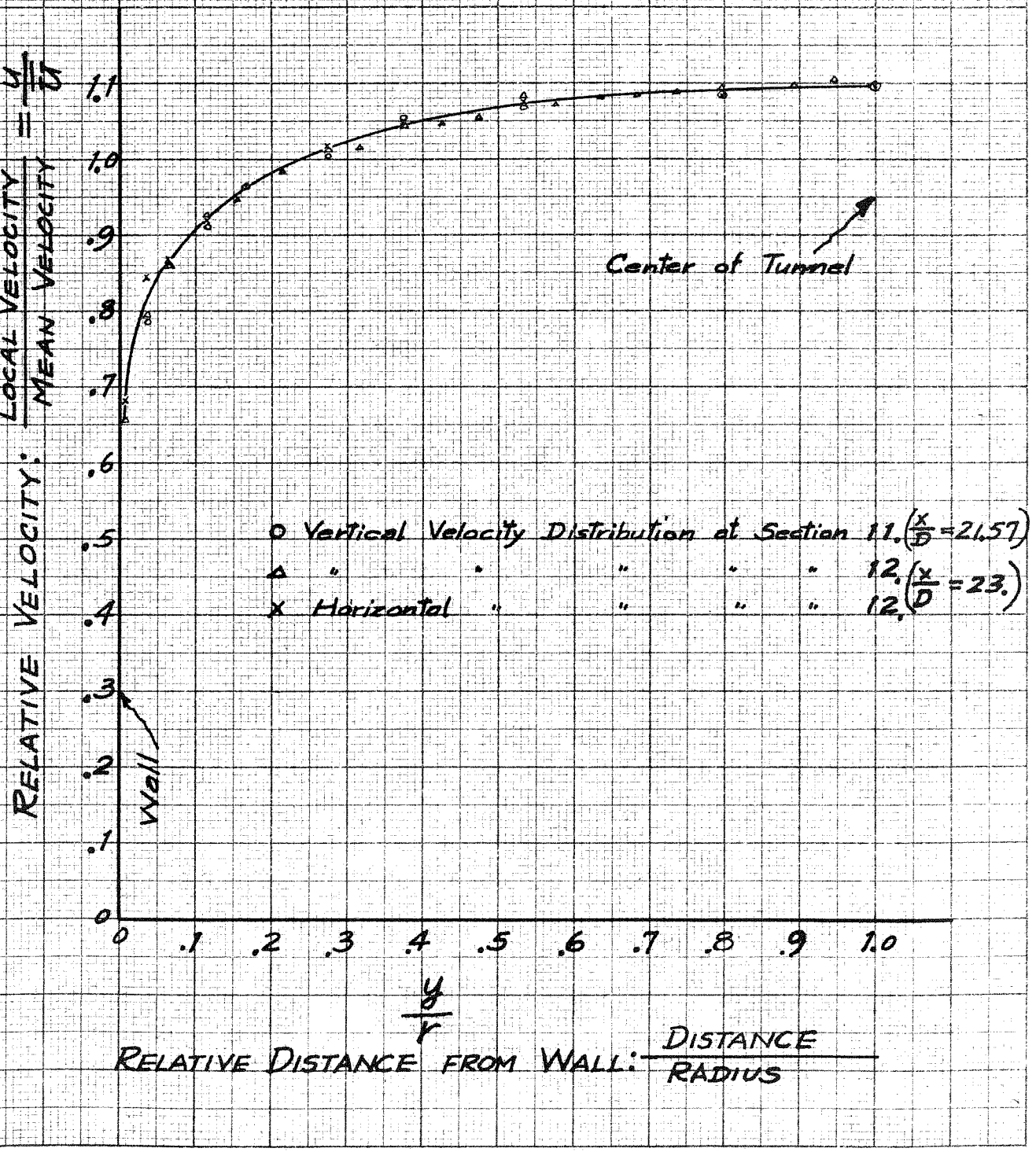

Diagram 25

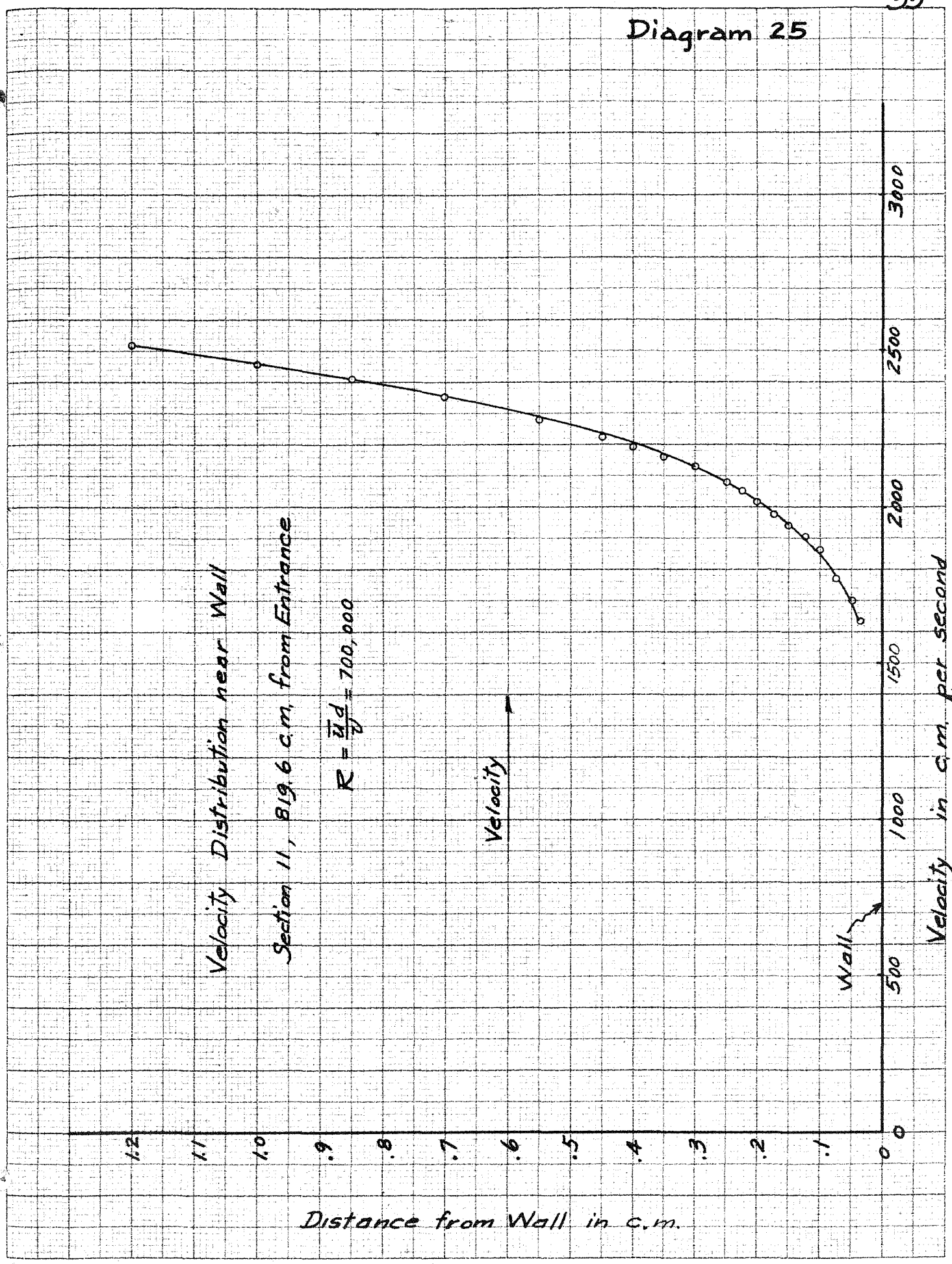
Velocity Distribution near Wall
Section 11, 819.6 c.m. from Entrance
$R = \frac{\bar{u}d}{\nu} = 700,000$
Velocity
Wall
Velocity in c.m. per second
0
500
1000
1500
2000
2500
3000
0
.1
.2
.3
.4
.5
.6
.7
.8
.9
1.0
1.1
1.2
Distance from Wall in c.m.

Diagram 26

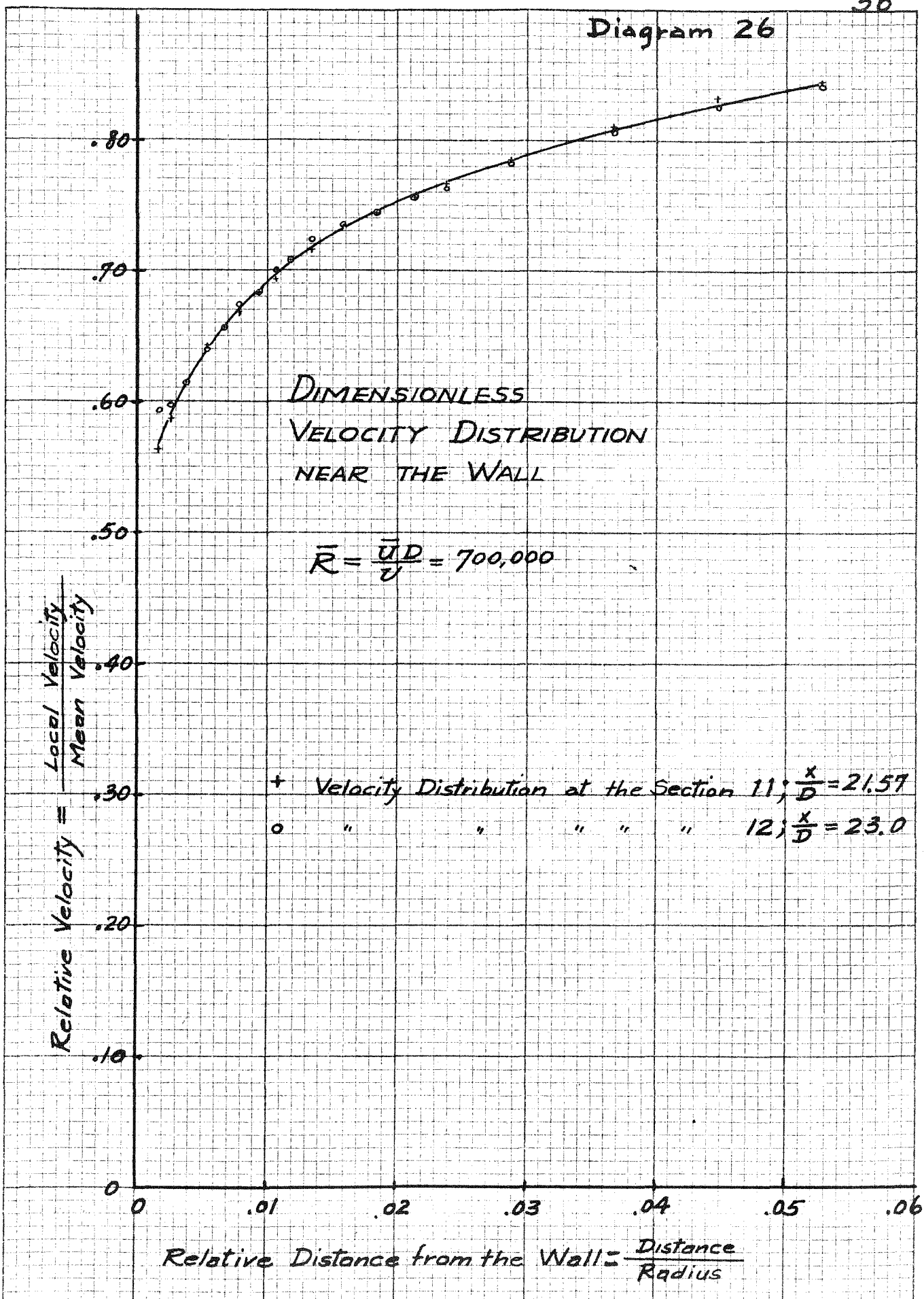
.80
.70
.60
.50
.40
.30
.20
.10
0
0
.01
.02
.03
.04
.05
.06
Relative Velocity = Local Velocity / Mean Velocity
Relative Distance from the Wall = Distance / Radius
DIMENSIONLESS
VELOCITY DISTRIBUTION
NEAR THE WALL
$\bar{R} = \frac{\bar{U}D}{\nu} = 700{,}000$
+ Velocity Distribution at the Section 11; $\frac{x}{D} = 21.57$
o " " " " " 12; $\frac{x}{D} = 23.0$

EXPERIMENTAL PROCEDURE AND RESULTS

Velocity distribution at sections 2-12 were measured using the large Pitot tube and the micromanometer with ethylene chlorohydrin, whose set up is as shown in the Fig. 7. The static pressure at the standard section was kept nearly constant within .4 mm. height of the fluid in all the measurements and less than .1 mm. height of the fluid during the measurement of any one of the sections. The data were corrected for gravity, density and temperature variations, using the Diags. 27-30, and reduced to velocity in cm. per second and plotted on the Diags. 10-21. For the purpose of comparison the velocity distributions at different sections were plotted non-dimensionally on the Diag. 22. Turbulent velocity distributions at the sections 11 and 12 were plotted on the same sheet to obtain the average value of the velocity distribution for a completely turbulent flow. (Diags. 23-26)

The power law of the velocity distribution is plotted on Diags 35 and 36. A comparison of the value of "n" obtained in this experiment and those obtained by Nikuradse and Möbius were plotted on the same sheet. (Diag. 37). Mischungsweg, using the formulae of Prandtl and Kármán were plotted on Diag. 38.

The Measurement of the Standard Pressure

The airflow through the tunnel was maintained nearly constant at all the measurements of the velocity distributions at the different tunnel sections. The regulation of the airflow was accomplished as follows:

The standard static pressure tube was connected to the standard pressure manometer as described on page 17, paragraph 3). The static pressure tube at the section 11 was connected to the manometer 1), page 17. The tunnel was then operated with motor running at its normal speed. The manometer 3) was then adjusted to register zero (its hairline just touching the bottom of the meniscus of the fluid), when the manometer connected to the static pressure tube at the section 11 read 7.670 cm. of the fluid height. This static pressure was taken to be the standard throughout the experiment and all the measurements were taken while the standard static pressure was nearly zero on the manometer 3). The regulation of the airflow to this static pressure at different times was made by adjusting the flow regulator located near the propeller, (Fig. 1).

SAMPLE CALCULATIONS

Velocity Distribution

Bernouli's equation gives,

$$H = p + \tfrac{1}{2}\rho v^2$$

where,
H---constant, total head,
p---static pressure at the point,
v---velocity,
ρ---density of the fluid.

When the static pressure tube is connected to one end of the manometer and the total head tube is connected to the other end, the manometer automatically measures the difference in term of the column of the fluid, then,

$$v = \sqrt{\frac{\Delta h \cdot 2\gamma}{\rho}}$$

where,
Δh---difference of the pressure head,
γ---specific gravity of the fluid.

The fluid used in this experiment was ethylene chlorohydrin, whose specific gravity was approximately 1.097. The density of the fluid was taken before every run. ρ varies with atmospheric pressure, temperature and gravity, and therefore, corrections were made for them. If we let ρ_1 be the corrected density of air, then we have

$$v = \sqrt{\Delta h}\sqrt{\frac{1.097 \times 2}{\rho_1}}$$

now let:

$$\Delta h = 4.915 \qquad \rho_1 = \frac{.00157}{980}$$

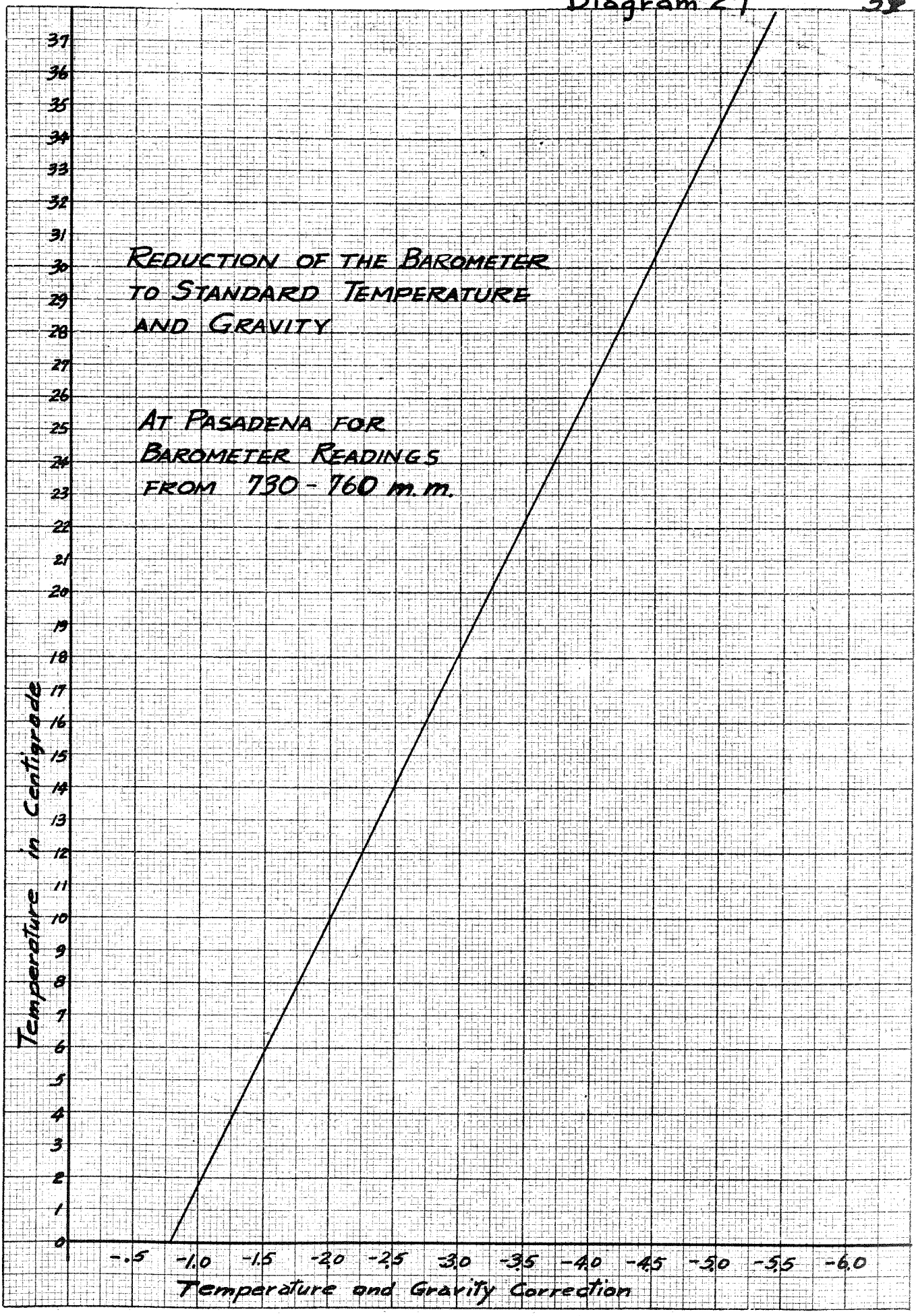
REDUCTION OF THE BAROMETER TO STANDARD TEMPERATURE AND GRAVITY
AT PASADENA FOR BAROMETER READINGS FROM 730 - 760 m.m.
Temperature in Centigrade
37
36
35
34
33
32
31
30
29
28
27
26
25
24
23
22
21
20
19
18
17
16
15
14
13
12
11
10
9
8
7
6
5
4
3
2
1
0
-.5
-1.0
-1.5
-2.0
-2.5
-3.0
-3.5
-4.0
-4.5
-5.0
-5.5
-6.0
Temperature and Gravity Correction

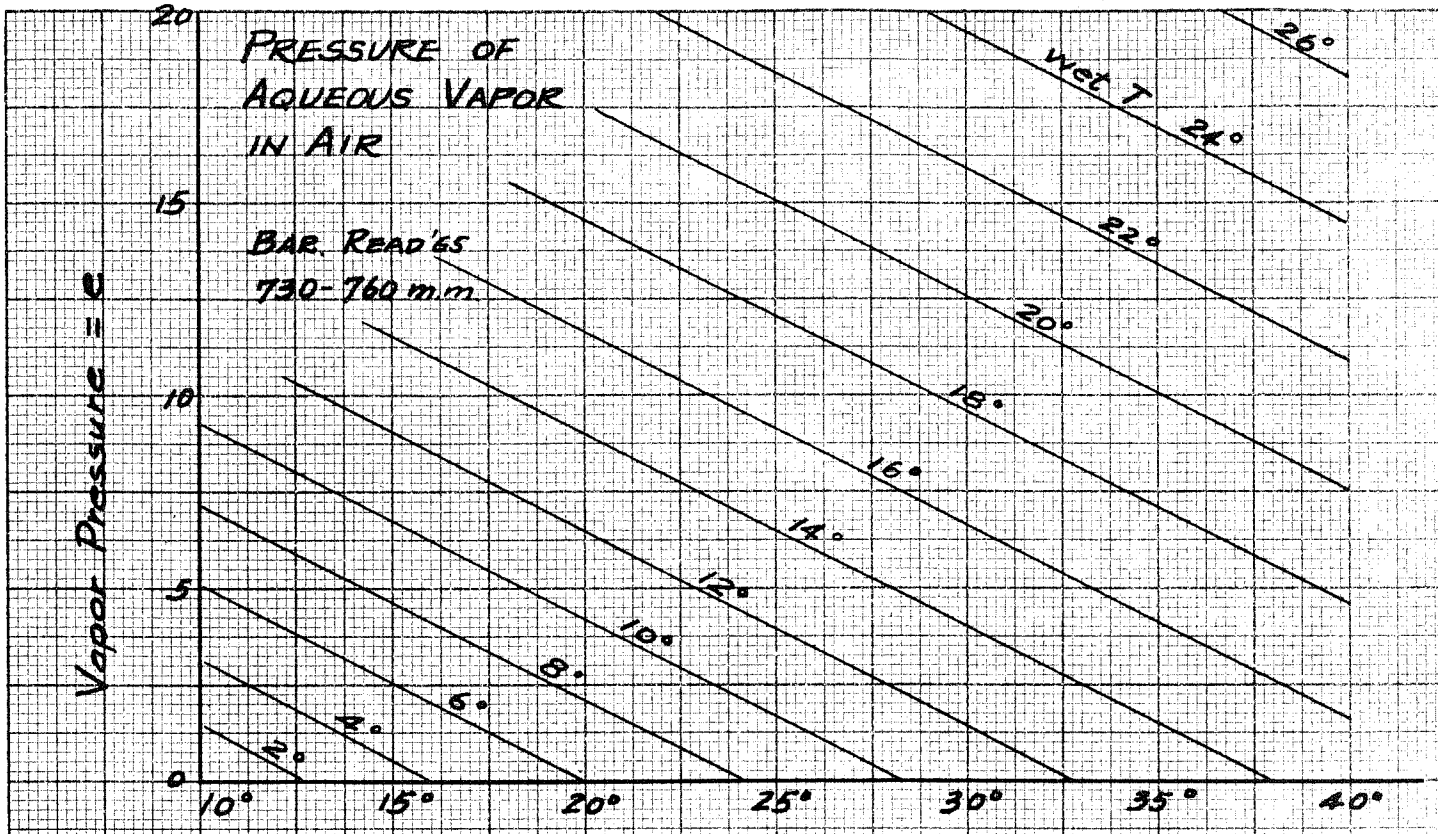

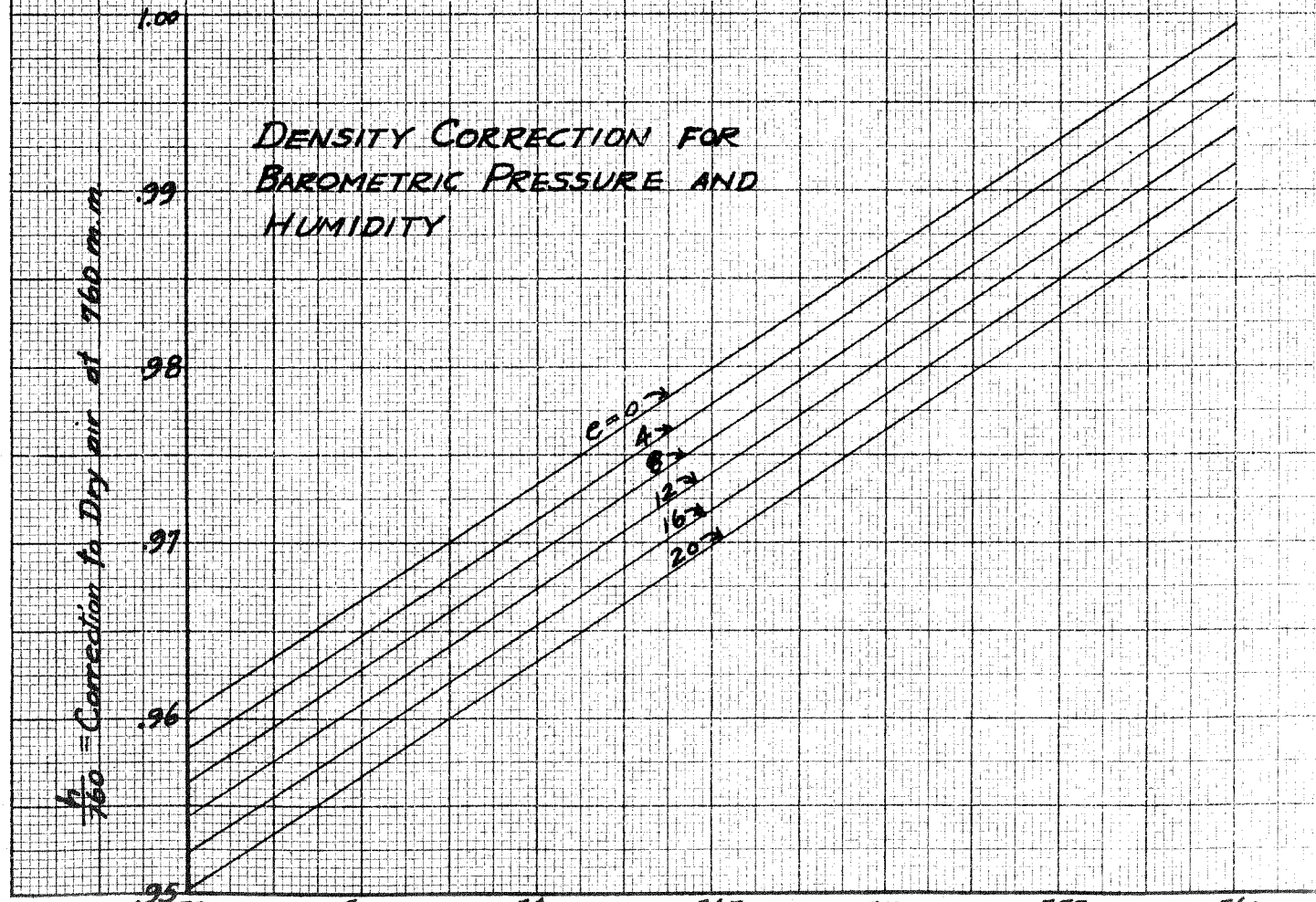

.00125

Diagram 29

Weight of Air including Aqueous Vapor

Corrected for Gravity "g" = 979.6

.0012

$\frac{b}{760} = 1.000$ .996 .992 .988 .984 .980 .976 .972 .968 .964 .960 .956 .954

.00115 $= p$

Weight of 1 c.c. of Air

.0011

10° 15° 20° 25° 30° 35° 4

Air Temperature (°C)

Diagram 30

KINEMATIC VISCOSITY OF AIR
INCLUDING AQUEOUS VAPOR

Corrected for "g" = 979.6

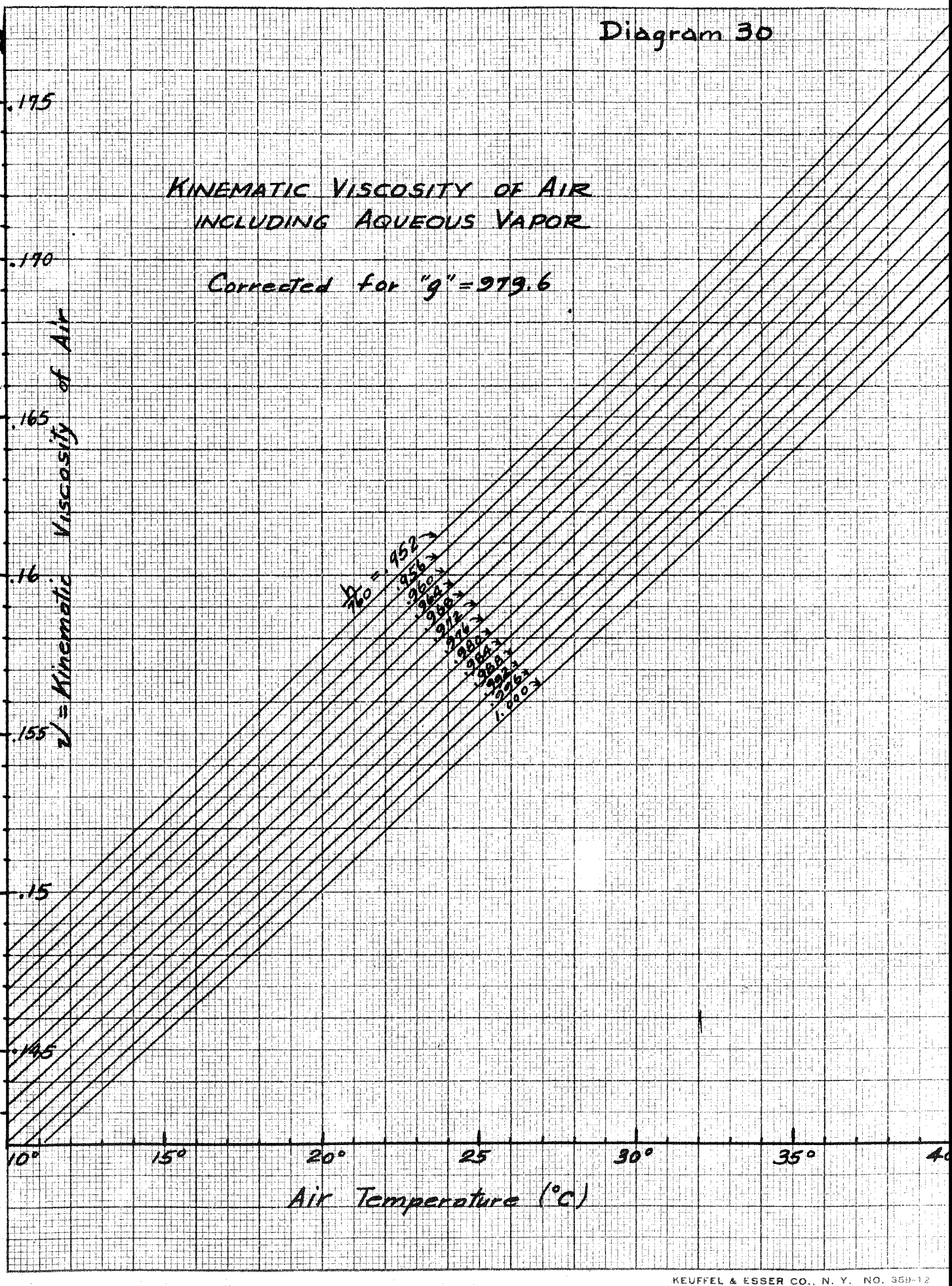

KEUFFEL & ESSER CO., N. Y. NO. 359-12
10 × 10 to the half inch.

then,

$$v = \sqrt{\Delta h}\sqrt{\frac{1.097 \times 2 \times 980}{.00157}} = \sqrt{4.915}\sqrt{\frac{1.097 \times 2 \times 980}{.00157}} = 3010 \text{ cm/sec.}$$

The correction for the density of air was made by means of charts in Diags. 27-30 inclusive.

Mean Velocity

The mean velocity is that velocity which multiplied by the area of the section gives the quantity of the air flow through the section. In a circular channel, the area of the section is given by,

$$\text{area} = \pi r^2$$ where, r--radius of the channel.

The quantity of the air flow through the section per second is given by,

$$Q = 2\pi \int_0^r v\, y\, dy$$

$$\bar{U}\pi r^2 = 2\pi \int_0^r v\, y\, dy$$

where,
y--distance from the center,
v---velocity of the flow at y cm. from the axis.
$\bar{U}$--mean velocity.

Now let:

$$y^2 = z \qquad 2y\,dy = dz$$

then,

$$Q = \pi \bar{U} r^2 = \pi \int_0^{z_1} v\, dz$$

$$r^2 = z_1 = y_1^2$$

$$\bar{U} = \frac{\int_0^{z_1} v\, dz}{z_1}$$

Therefore, to obtain the mean velocity, using the average velocity distribution curve of the Diag. 23, the velocity was

plotted on y^2 scale. (Diag. 31). The enclosed area was measured by means of a planimeter, and this area was then divided by the actual distance on the Diag. 31 between the 0 velocity and the maximum velocity. This gave the distance on the Diag. 31 corresponding to the mean velocity. This velocity was then read on the scale. The mean velocity was found to be 2900 cm./sec.

Wall Friction and Shearing Stress

In the equation (9)

$$\tau_o = \frac{dp}{dx}\,\frac{r}{2} \qquad r = 19 \text{ cm.}$$

$\frac{dp}{dx}$ was calculated from the experiment. According to the Diag. 9 dp/dx was found to be .00173 cm. of water per one cm. of length. Therefore,

$$\frac{dp}{dx} = .00173 \text{ cm. of water}$$

$$= .00173 \cdot 980 = 1.695 \text{ dynes/ cm. of channel length.}$$

$$\tau_o = \frac{1.695 \times 19}{2} = 16.09$$

Therefore,

$$\frac{\tau_o}{\rho_1} = \frac{16.09}{.001145} = 14.000 \qquad \rho_1 = .001145$$

$$\tau = \tau_o \frac{y}{r} \qquad (10)$$

The above equation (10) is a linear function in which τ is maximum at the wall and approaches 0 at the center. The value of τ, the shearing stress as function of y was plotted on Diag. 32.

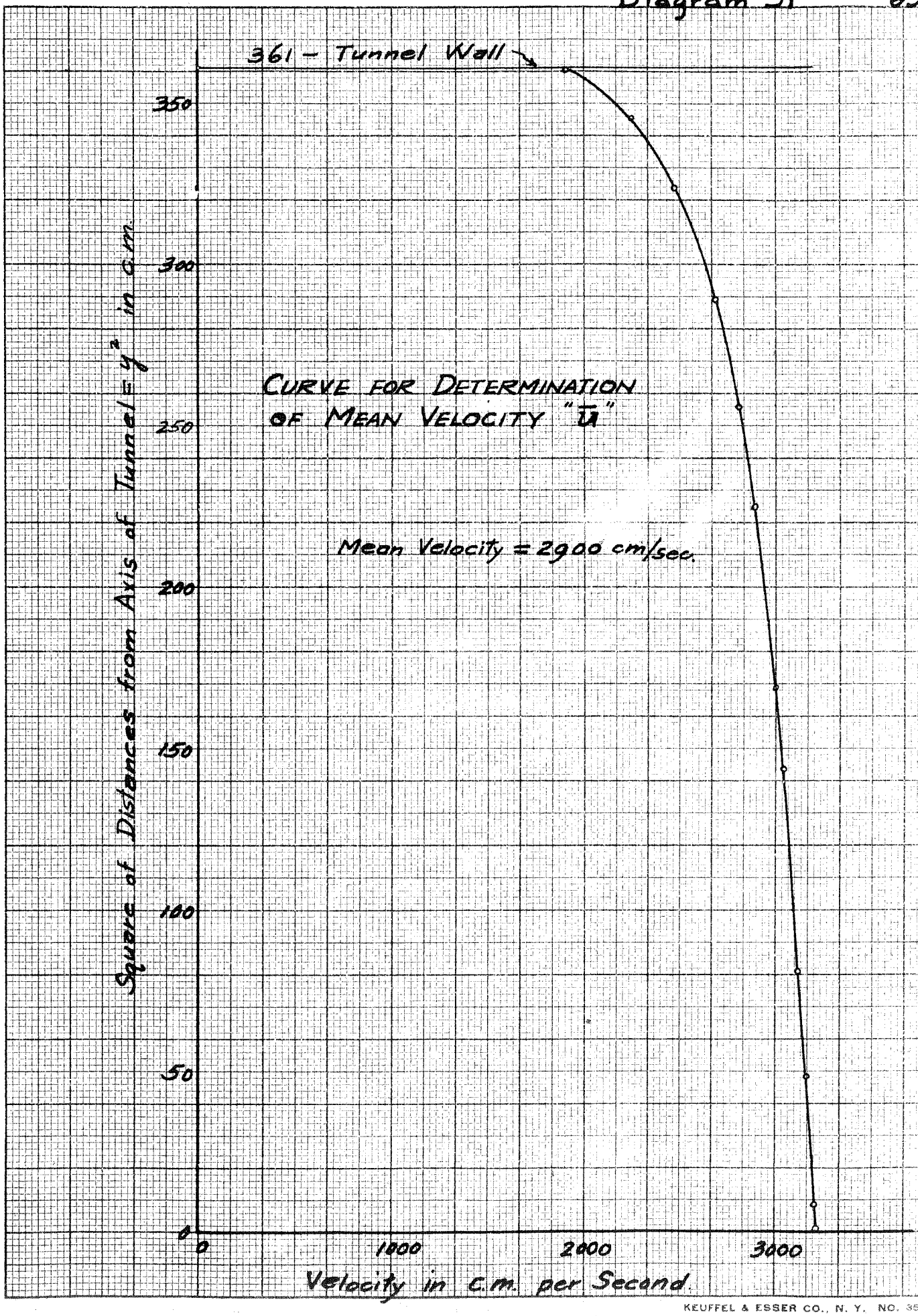

KEUFFEL & ESSER CO., N. Y. NO. 359-12
10 to the half inch.

Diagram 32

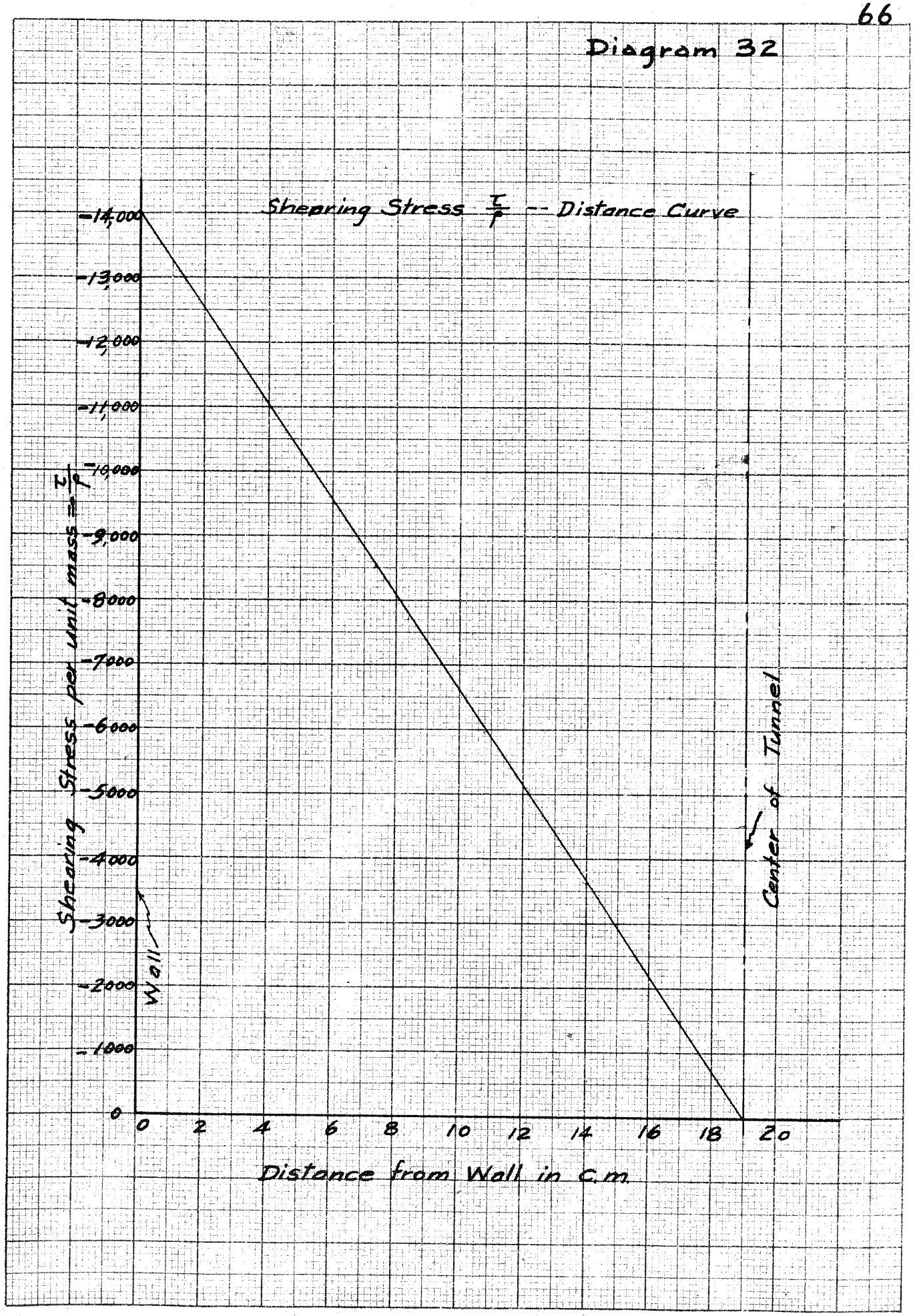
Shearing Stress $\frac{T}{\rho}$ -- Distance Curve
Shearing Stress per unit mass $= \frac{T}{\rho}$
-14,000
-13,000
-12,000
-11,000
-10,000
-9,000
-8000
-7000
-6000
-5000
-4000
-3000
-2000
-1000
0
Wall
Center of Tunnel
0
2
4
6
8
10
12
14
16
18
20
Distance from Wall in C.m.

Calculation of Mischungsweg

Using the equation (4) and (11), mischungsweg distribution was calculated. In this calculation the slope of the turbulent velocity distribution curve and also the slope of the above slope were necessary. (Diags. 33 and 34). Using the values on the above curves, it was then an easy matter to calculate the values of mischungsweg. The values of $\frac{\tau}{\rho}$ were obtained from the Diag. 32. In order to make the values dimensionless, the mischungsweg was divided by the radius of the tunnel. The distribution curves in a dimensionless form were plotted on the Diag. 38.

Diagram 33

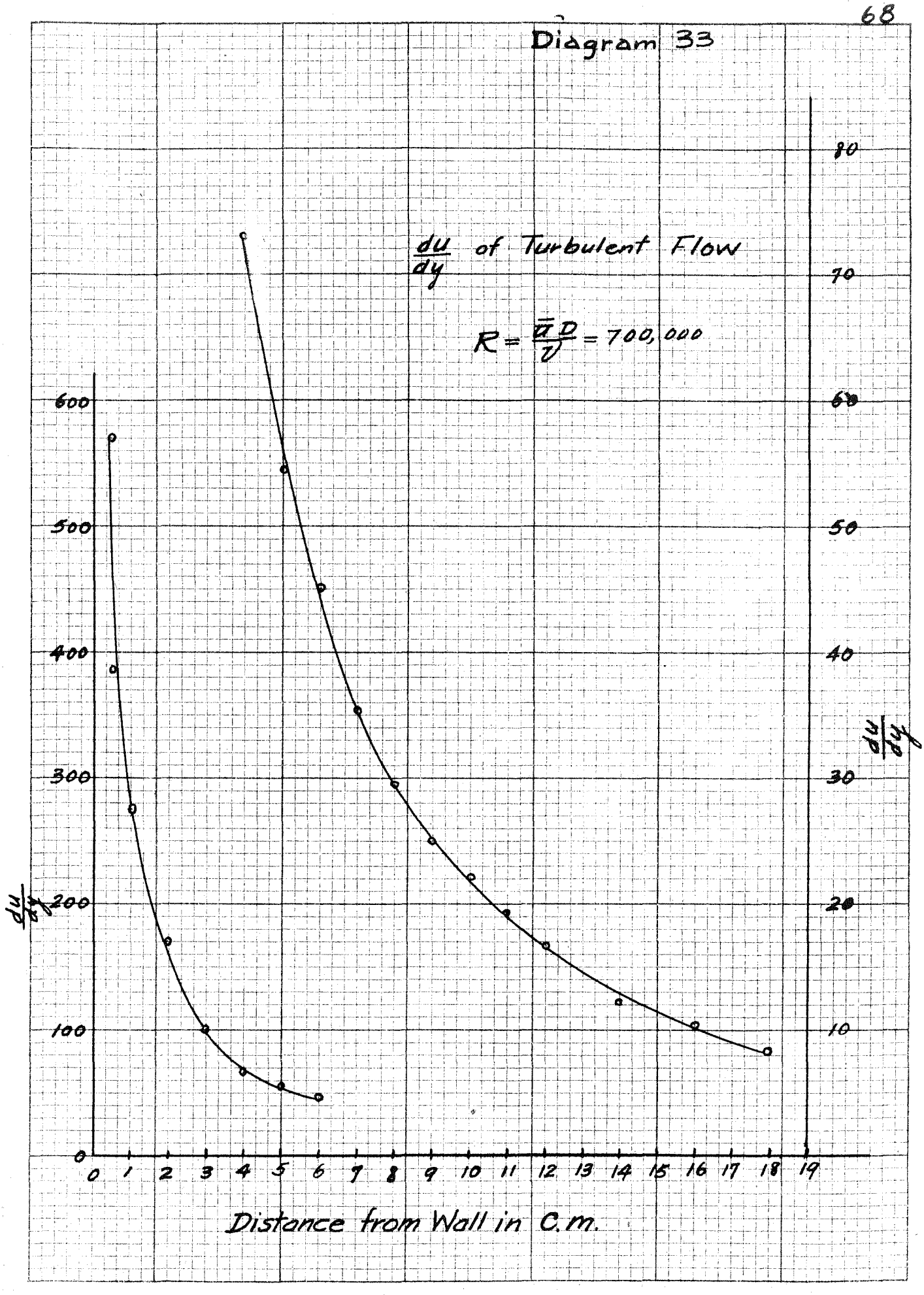
du/dy of Turbulent Flow
R = ū D / ν = 700,000
600
500
400
300
200
100
0
du/dy
80
70
60
50
40
30
20
10
du/dy
0 1 2 3 4 5 6 7 8 9 10 11 12 13 14 15 16 17 18 19
Distance from Wall in C.m.

Diagram 34

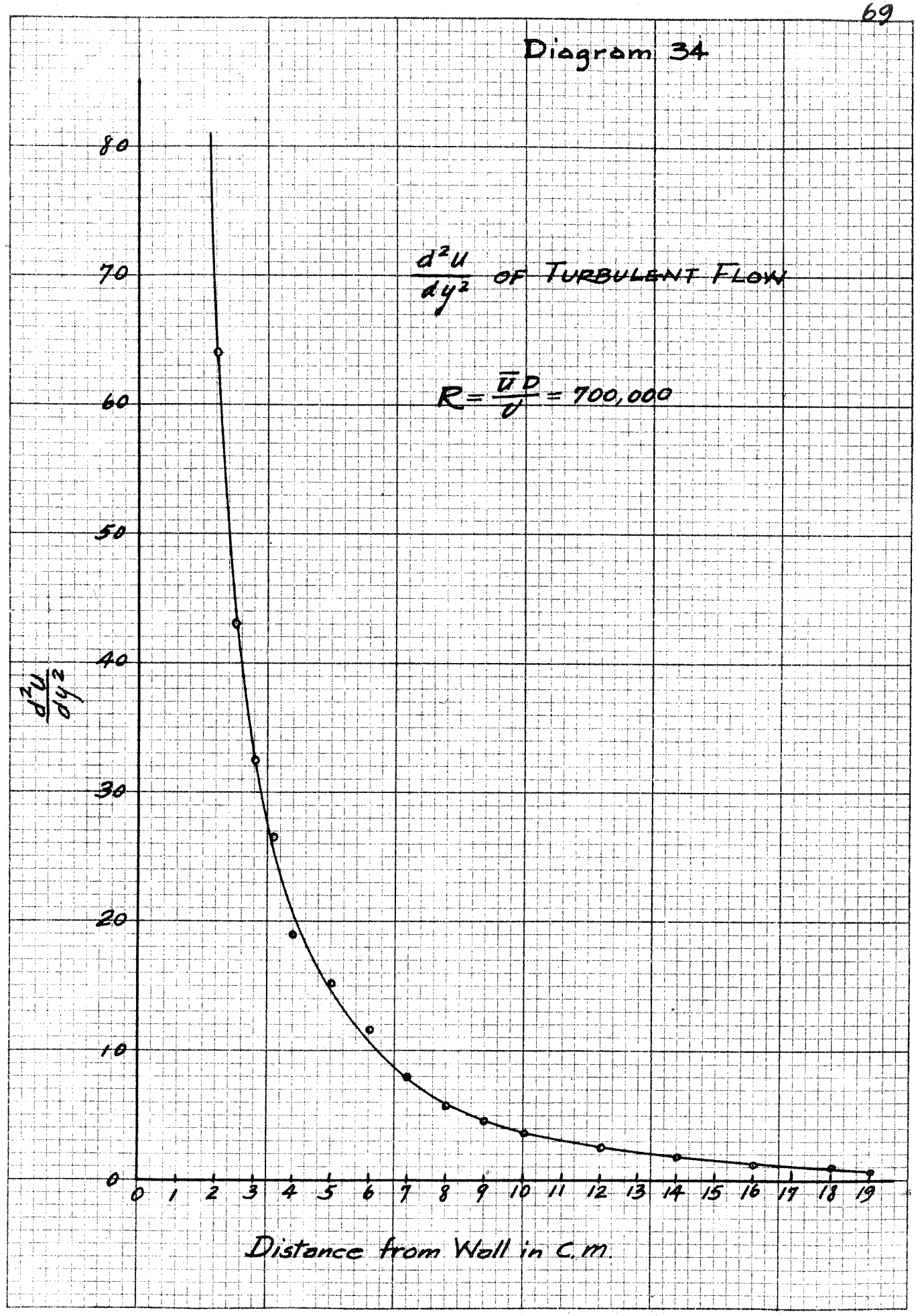
$\frac{d^2u}{dy^2}$ OF TURBULENT FLOW
$R = \frac{\bar{u} D}{\nu} = 700,000$
$\frac{d^2u}{dy^2}$
80
70
60
50
40
30
20
10
0
0 1 2 3 4 5 6 7 8 9 10 11 12 13 14 15 16 17 18 19
Distance from Wall in C.m.

DISCUSSION OF THE RESULTS

The velocity distributions at the sections 2, 3, 4, and 5 are very much distorted, but after the section 6, the distribution is symetrical. At the section 6, there is a definite peak at the center of the tunnel, indicating that the boundary layers from the opposite walls have met. This is also confirmed by the Diag. 9, in which we note that the constant slope of the total head drop begins at the section 6. The velocity distribution of the flow after the boundary layers have joined, from the Diags. 22, 14-21, remains unchanged and has the same form, within the limit of the experimental error.

The great dissymetry of the velocity distribution near the entrance may be attributed to the bluntness of the entrance and to the probable distorsion of the air current before the entrance. However, even such a great unevenness of the distribution, after a short distance, specifically approximately 10 diameters from the entrance, the flow became symetrical and completely turbulent. "Anlauf", the distance from the entrance to the point where the flow becomes completely turbulent, depends largely upon the type of the entrance condition.

In the dimensionless curves, the velocity at various points were divided by the mean velocity instead of the maximum velocity as usually is done, because the maximum velocity at various sections differ, while the mean velocity remains the same because of the continuity condition, that equal amount of air must be flowing through all the sections at the same instant. The cross-sectional areas at all the sections are

Diagram 35

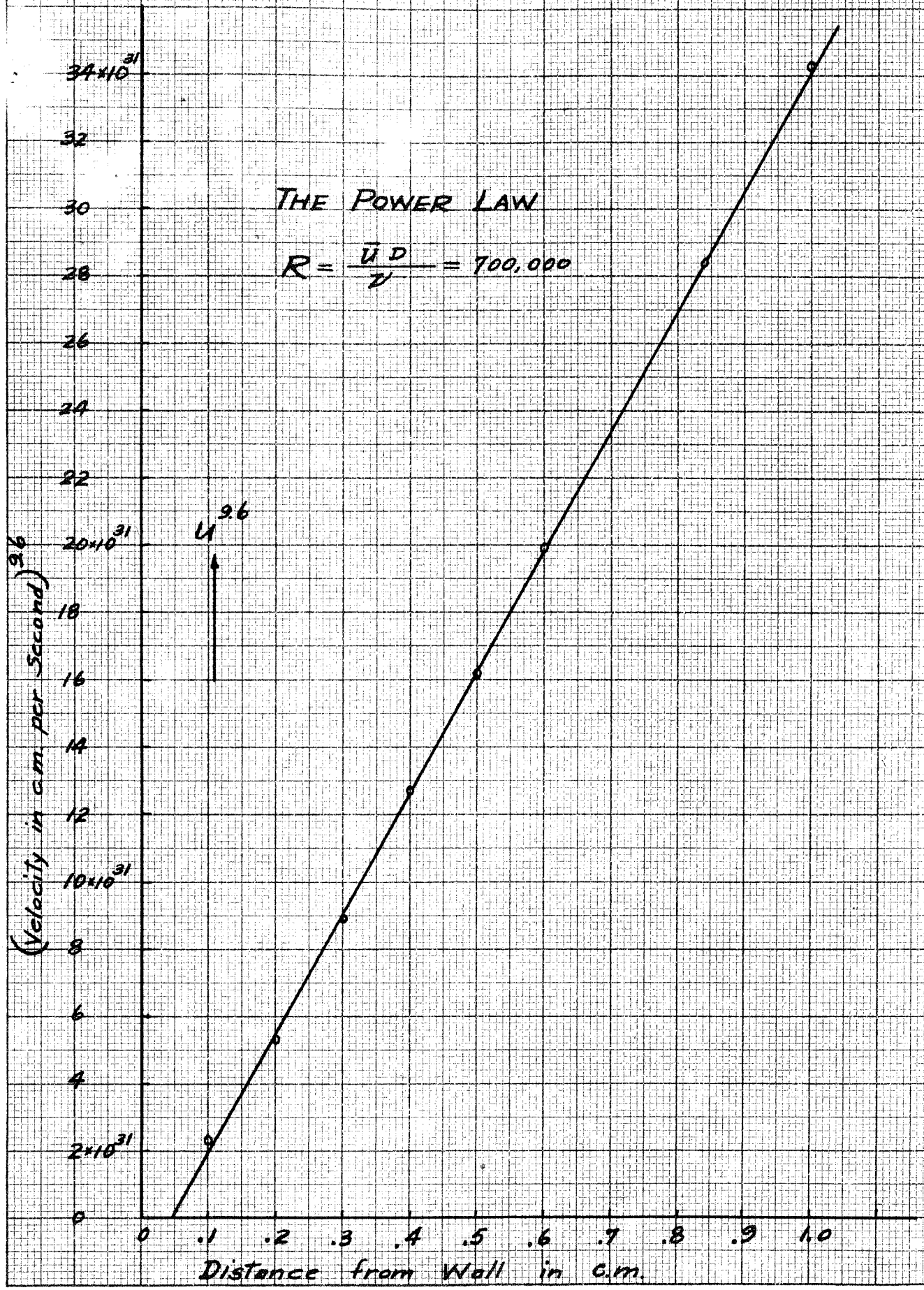

KEUFFEL & ESSER CO., N. Y. NO. 359-12
10 × 10 to the half inch.

Diagram 36

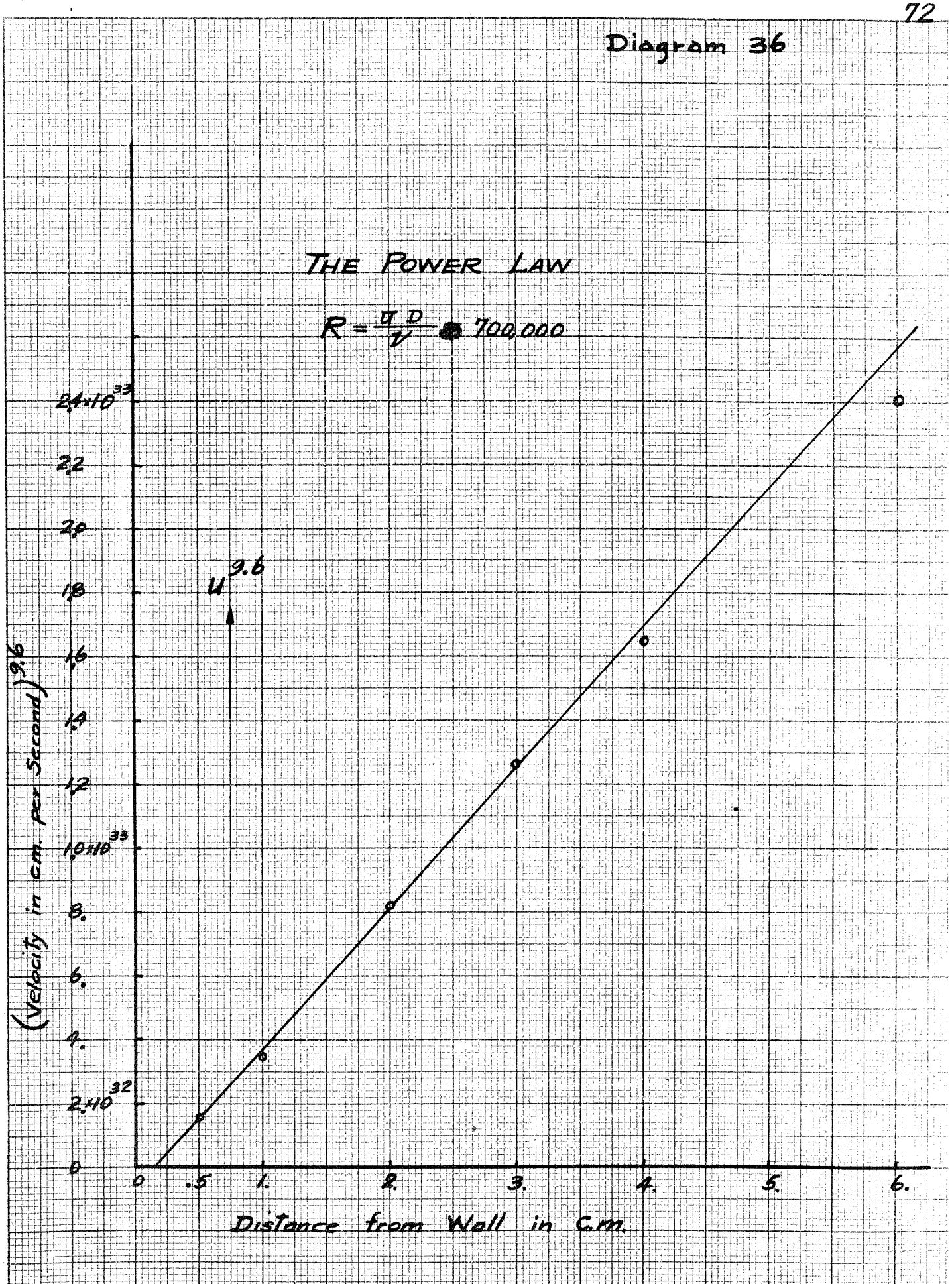

equal and hence the mean velocity must be equal at all the sections.

The velocity distribution curve of the turbulent flow as plotted on the Diags. 24 and 26 are the average of the velocity distribution measurements at two different sections. In a completely developed turbulent flow, the velocity distribution curve should have the same shape. This theory is well verified by the fairly good congruency of the points measured at the two sections.

The value of "n", the velocity distribution power coefficient as determined by the present experiment agrees well with the previous experiments and falls on the curve drawn through the measurements of Nikuradse and Möbius as shown on the Diag. 37.

The mischungsweg distribution has been calculated using Prandtl formula $\left(\frac{l}{r} = \frac{\sqrt{\frac{\tau}{\rho}}}{r\frac{du}{dy}}\right)$ and Kármán formula $\left(\frac{l}{r} = \frac{\kappa}{r}\frac{\frac{du}{dy}}{\frac{d^2u}{dy^2}}\right)$ and plotted on the same sheet on which is drawn a curve according to Kármán's $\left(\frac{l}{r} = 2\kappa\left\{\sqrt{1-\frac{y_1}{r}} + \frac{y_1}{r} - 1\right\}\right)$ formula. The ~~xxx~~ first curve falls above and the second curve falls below the third curve. All the three curves agree well near the wall, but toward the center they deviate quite radically. In this experiment, the tunnel used was made of sheet metals, and was not very accurately circular because of the difficulty in construction. This distorsion of the supposedly circular tunnel caused the Pitot tube to occupy the position somewhat further from the center than was assumed. Hence the readings were slightly low. The mischungsweg calculated using the slope of the distribution curve, is slightly erraneous toward the center, because the du/dy term occurs in the denominator in

Diagram 37

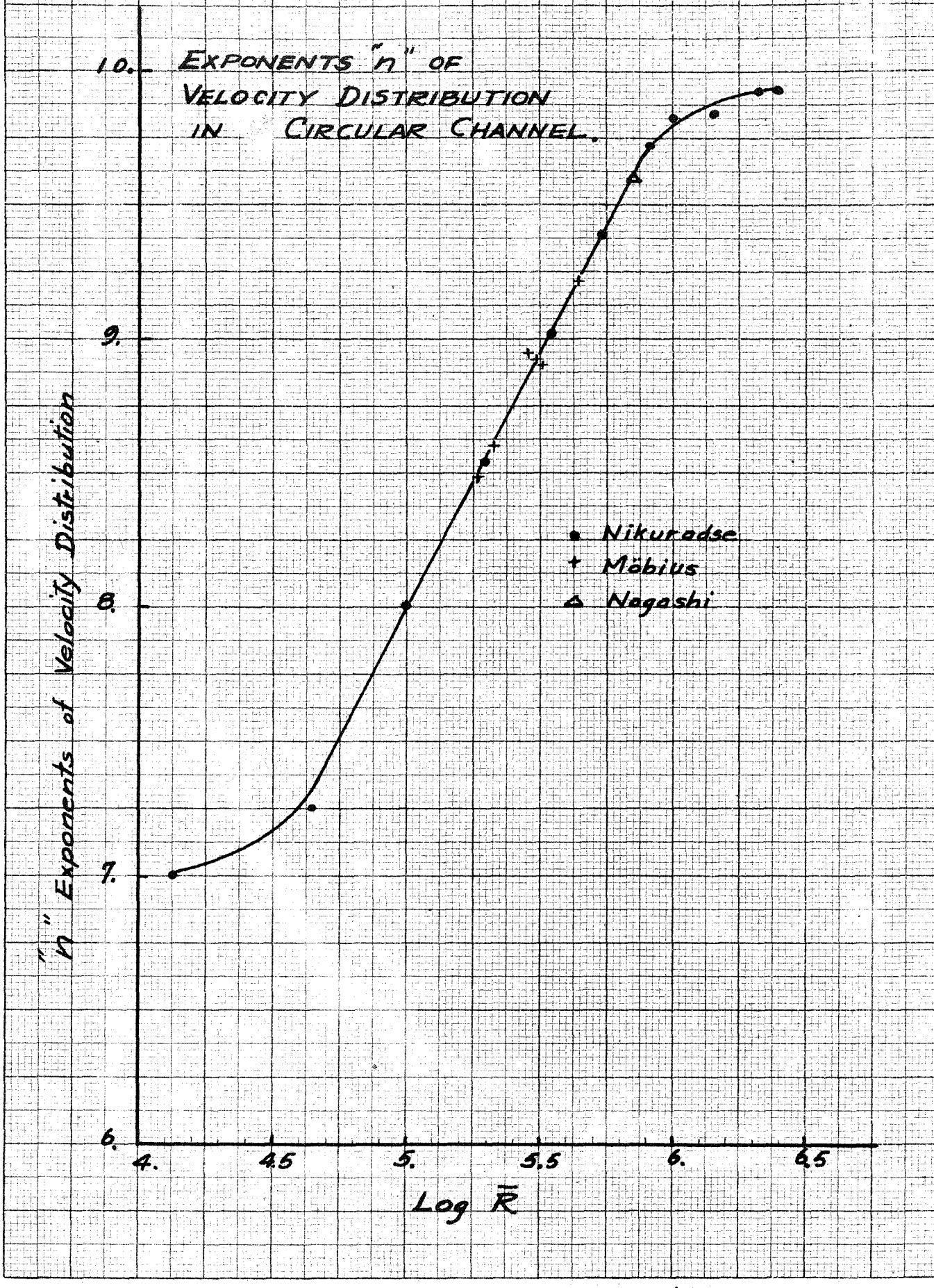
EXPONENTS "n" OF
VELOCITY DISTRIBUTION
IN CIRCULAR CHANNEL.
10.
9.
8.
7.
6.
"n" Exponents of Velocity Distribution
Nikuradse
Möbius
Nagashi
4.
4.5
5.
5.5
6.
6.5
Log R̄

Diagram 38

DIMENSIONLESS MISCHUNGSWEG DISTRIBUTION

$$R = \frac{\bar{u} D}{\nu} = 700{,}000$$

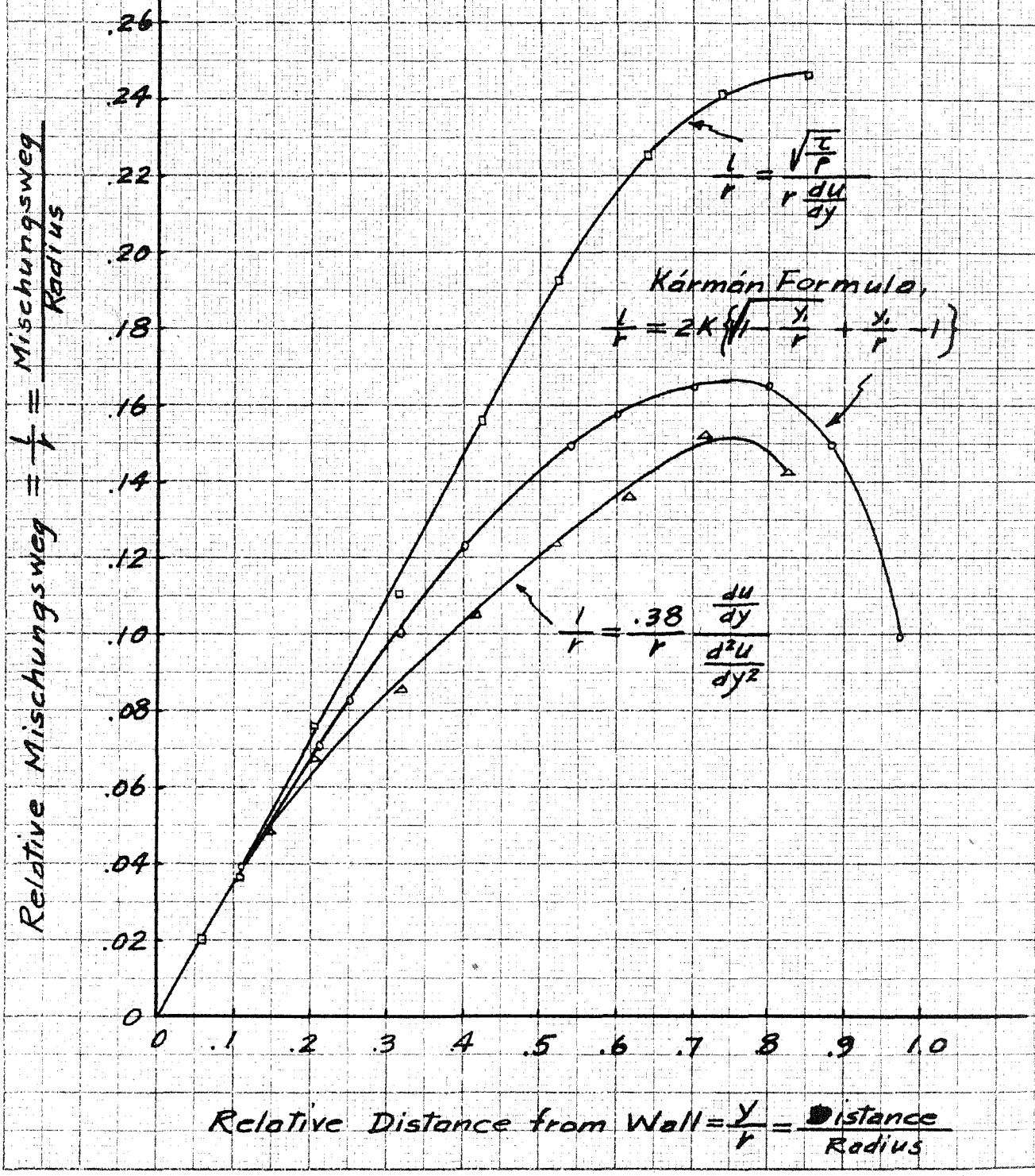

the Prandtl formula and in the numerator in the Kármán formula.

In the future experiments care should be taken to choose a tunnel that is as nearly circular as possible to avoid similar source of error. Judging by the results of this experiment, however, the Kármán formula of mischungsweg as function of y gives in a rough way fairly accurate mischungsweg distribution.

In conclusion, the author wishes to express his gratitude to the various members of the Aeronautics Department of the California Institute of Technology for their assistance in carrying out the experiment, especially to Dr. W. Tollmien for the kind guidance and helpful suggestions given him during the progress of the experiment, to Mr. Frank Wattendorf for his assistance in taking measurements and for the use of the micrometer for the Pitot tube, to Dr. Arthur Klein for his helpful suggestions in designing the measuring instruments, and to Dr. Theodor von Kármán and Dr. Clark B. Millikan for suggesting this problem and for giving many constructive suggestions to the author.

BIBLIOGRAPHY

1) Prandtl, Ludwig. Nachrichten von der Gesellschaft der Wissenschaften zu Göttingen, Mathematisch-physikalische Klasse, 1914. p. 177

2) Blasius, H. Zeitschrift fur Mathematik und Physik, 1908, v. 56: 1-37

3) Boltze, E. Göttingen Disertation, 1908.

4) Hiemenz, K. Die Grenzschicht an einem in den gleichformigen Flussigkeitsstrom eingetauchten geraden Kreiszylinder. Dinglers Polytechnisches Journal, 1911, v. 326: 321-24.

5) von Kármán, Th. Uber laminare und turbulente Reibung. Zeitschrift fur Angewandte Mathematik und Mechanik, 1921 v. 1:233-252.

6) Schiller, L. Die Entwicklung der laminaren Geschwindigkeitsverteilung und ihre Bedeutung fur Zähigkeitsmessungen. Zeitschrift fur Angewandte Mathematik und Mechanik, 1922, v. 2:96.

7) Nikuradse, J. Untersuchungen uber die Stromungen des Wassers in konvergenten und divergenten Kanalen. Forschungsarbeiten auf dem Gebiete des Ingenieurwesens. Berlin, 1929, heft 289. p. 49.

8) Dönch, F. Divergente und konvergente turbulente Stromungen mit kleinen Öffnungswinkeln. Forschungsarbeiten auf dem Gebiete des Ingenieurwesens, 1926, heft 282.

9) Hansen, M. Die Geschwindigkeitsverteilung in der Grenzschicht an einer eingetauchten Platte. Zeitschrift fur Angewandte Mathematik und Mechanik, 1928, v. 8:185-199. (Translation: N.A.C.A. Tech. Mem. No. 585)

10) van der Hegge Zijnen, B. G. Experiments on the Velocity Distribution in the Boundary Layer along a Rough Surface, Determination of the Resistance Experienced by This Surface. K. Akademie van Wetenschappen, Amsterdam, Proceedings. 1927, v. 31:499-518.

11) Tollmien, W. Uber die Entstehung der Turbulenz. Nachrichten von der Gesellschaft der Wissenschaften zu Göttingen. Mathematisch-physikalische Klasse, 1929, heft 1. (Translation: N.A.C.A. Tech. Mem. No. 609. p. 27)

12) Schiller, L. und Herman, R. Widerstand von Platte und Rohr bei hohen Reynoldsschen Zahlen. Ingenieur Archiv. September 1930, p. 391-398. Translation: N.A.C.A. Tech. Mem. No. 600)

13) von Kármán, Th. Mechanische Ahnlichkeit und Turbulenz, Nachrichten von der Gesellschaft der Wissenschaften zu Göttingen, Mathematisch-physikalische Klasse, 1930. (Translation: N.A.C.A. Tech. Mem. No. 611)

14) Prandtl, L. On the Roll of Turbulence in Technical Hydrodynamics. Tokyo World Engineering Congress. 1929.

15) Prandtl, L. Bericht uber Untersuchungen zur ausgebildeten Turbulenz. Zeitschrift fur Angewandte Mathematik und Mechanik, 1925, v. 5.

16) Prandtl, L. Uber die ausgebildete Turbulenz. Proceedings of the Second International Congress for Applied Mechanics, Zurich, 1926. (Translation: N.A.C.A. Tech. Mem. No. 435)

17) Stanton, E. T. and Pannell, J. R. Similarity of Motion in Relation to the Surface Friction of Fluids. Philosophical Transactions of the Royal Society of London, ~~1924~~ 1914 v. 214 A. p. 199.

18) Stanton, E. T. The Mechanical Viscosity of Fluids. Proceedings of the Royal Society of London, 1911 v. 85 A. p. 366.

19) Nikuradse, J. Untersuchung uber die Geschwindigkeitsverteilung in turbulenten Strömungen. Forschungsarbeiten auf dem Gebiete des Ingenieurwesens, 1926, heft 281.

20) Nikuradse, J. Uber turbulente Wasserstromungen in geraden Rohren bei sehr grossen Reynoldsschen Zahlen. Vertrege aus dem Gebiete der Aerodynamik und verwandter Gebiete. Aachen 1929.

21) Jacob, M, und Erk, S. Der Druckabfall in glatten Rohren und die Durchflussziffer von Normaldüsen. Forschungsarbeiten auf dem Gebiete des Ingenieurwessens, 1924, heft 267.

22) Hopf, L, and Fromm, K. Die Messung der hydraulischen Rauhigkeit. Zeitschrift fur angewandte Mathematik und Mechanik, 1923 v. 3. p. 329.

23) Frisch, W. Der Einfluss der Wandrauhigkeit auf die turbulente Geschwindigkeitsverteilung in Rinnen. Zeitschrift fur angewandte Mathematik und Mechanik, 1928, v. 8, p. 199.

24) Schiller, L. Rohrwiderstand bei hohen Reynoldsschen Zahlen. Vorträge aus dem Gebiete der Aerodynamik und verwandter Gebiete, Aachen 1929.